Renewable and Sustainable Energy Reviews 91 (2018) 962–986

Contents lists available at ScienceDirect

Renewable and Sustainable Energy Reviews

journal homepage: www.elsevier.com/locate/rser

Review and comparative study of single-stage inverters for a PV system

Ankit[a], Sarat Kumar Sahoo[a,*], Sukruedee Sukchai[b], Franco Fernando Yanine[c]

[a] School of Electrical Engineering, VIT University, Vellore, India
[b] School of Renewable Energy Technology (SERT), Naresuan University, Phitsanulok Thailand
[c] School of Engineering of Universidad Finis Terrae, Providencia, Santiago, Chile

ARTICLE INFO

Keywords:
Single stage inverter
Grid connected inverter
MPPT
Boost inverter

ABSTRACT

Energy from the sun is harnessed through a photovoltaic (PV) array in form of DC. This available DC voltage is converted into AC for industrial or domestic use as per the requirement. In some topologies the extracted DC voltage is stepped up to a higher level of DC using a boost or a buck-boost converter and then this stepped up DC voltage is converted into AC by the use of an inverter. However this process is pretty costly because of the larger number of components employed. An efficient alternative to this two-stage approach is the Single-Stage Inverter (SSI). SSI does the boosting of DC and inversion of the DC to AC using only a single circuit and hence the name Single-Stage Boost Inverter. SSBI give us the advantage of reduced and robust circuitry along with reliability and efficiency. This paper presents a review of the various (however not all) SSI topologies in PV systems.

1. Introduction

With the surge in demand for electrical energy globally [1], conventional (non-renewable) energy sources are being harnessed at a very rapid rate and pretty soon the mankind would run out these resources. The use of conventional energy sources also leads to the pollution of environment. Fig. 1a) shows a comparison between the electricity produced globally and between India, Fig. 1b). shows the coal and lignite production worldwide and in India, Fig. 1c). presents the CO2 emissions throughout the world and in India over the years from 1990 to 2015.

However, with the advancements in technology, the human race has been able to harness the non-conventional (renewable) energy resources such as the wind, solar, geothermal or hydro. The non-conventional energy resources have several advantages over the conventional energy resources such as

a) These resources are abundant in nature
b) These are very easily available etc.

By far the biggest advantage these non-conventional resources have over the conventional fossil fuels is that the former are a cleaner source of energy with no hazardous byproducts. When a comparison is done between the various renewable sources it is found that solar energy is the best option among the category. Hydro plants require a large investment in terms of capital, land and manpower. Wind power plants cannot be installed everywhere and availability of constant wind all the time can also not be guaranteed. Other options such as geothermal energy or tidal energy require sophisticated and costly technology to harness energy. Considering all the pros and cons of the several non-renewable energy options available, solar energy tops the list. Solar energy is put to commercial or household use by first converting the sun light into DC by the help of PV array and then this DC can be converted into AC and fed to the grid or run an independent load such as street lights or water pumps for irrigation etc. Since the PV output depends on solar irradiation and the ambient temperature, to extract maximum power from the PV module maximum power point tracking (MPPT) is used as a control technique [2]. Based on the number of power processing stages PV inverters can be put under two different categories multi-stage inverters and single-stage inverters. A multi stage inverter employs more than one power processing stage [3] where in one or many stages achieve the task(s) of boosting the DC output from PV array and/or galvanic isolation with the final stage being the conversion of the boosted DC into high-quality AC. However most of the PV inverters employ a two-stage power conversion process [4–6]. During the initial stage, PV array output is increased to a higher level with the help of a DC-DC boost converter while tracking maximum solar power, and during the second stage this DC is converted into AC power of high quality. Even though these two stage inverters have been in existence for a while and work well, but due to a higher number of part count they have a drawback of lower efficiency along with higher costs, bigger size and low reliability. Considering the aforementioned drawbacks of both multi-stage and two stage inverters, single-stage inverters which boost the PV output, employ MPPT and invert the boosted DC

* Corresponding author.
E-mail addresses: ankit.m@vit.ac.in (Ankit), sksahoo@vit.ac.in (S.K. Sahoo), sukruedeen@nu.ac.th (S. Sukchai), fyanine@uc.cl (F.F. Yanine).

https://doi.org/10.1016/j.rser.2018.04.063
Received 24 March 2017; Received in revised form 1 September 2017; Accepted 14 April 2018

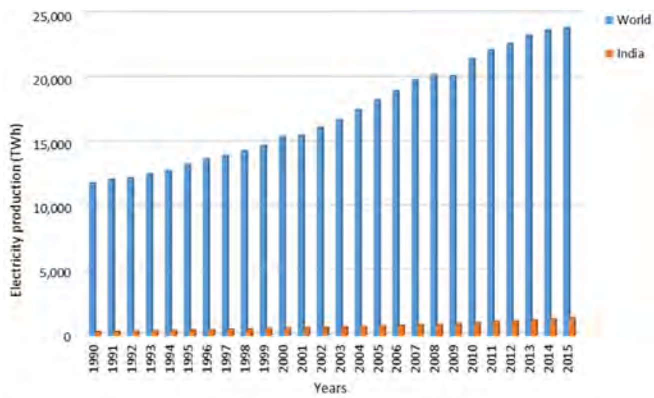

a). Electricity production (TWh) from 1990 to 2015 across World and India [1].

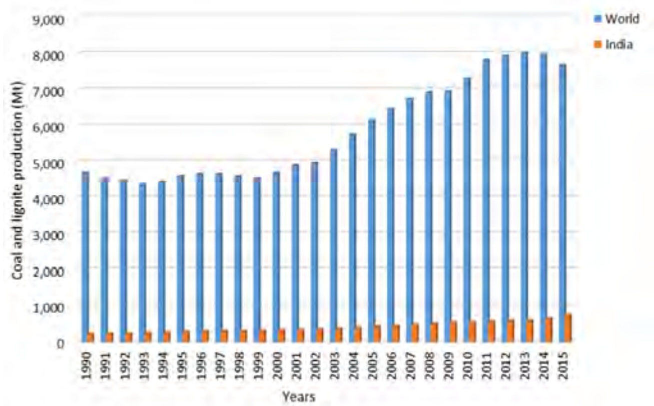

b). Coal and lignite production (Mt) from 1990 to 2015 across World and India [1].

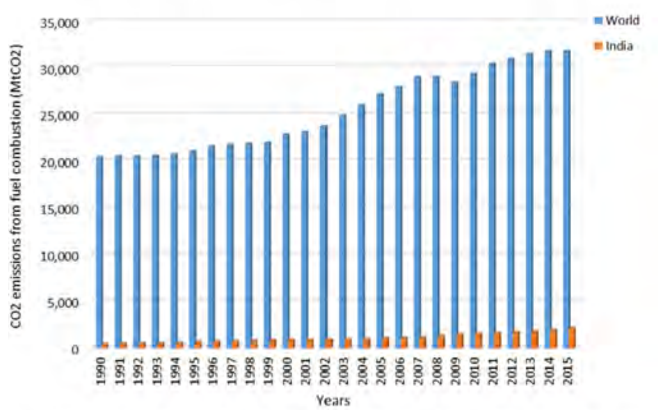

c). CO2 emissions from fuel combustion (MtCO2) from 1990 to 2015 across World and India [1].

Fig. 1. a). Electricity production (TWh) from 1990 to 2015 across World and India [1], b). Coal and lignite production (Mt) from 1990 to 2015 across World and India [1], c). CO2 emissions from fuel combustion (MtCO2) from 1990 to 2015 across World and India [1].

into AC using only a single power electronic circuit are becoming popular these days. SSI is a circuit (Fig. 2.) which can convert a low-level DC voltage and convert this low DC input into AC output of commercial quality. Fig. 3. is also an SSI in which an unfolding bridge converts the boosted DC into commercial AC [7]. There are a lot of reviews on various topics related to renewable energies such as grid connected PV systems [8–14], wind energy [13,15] and MPPT [16,17] etc. but so far there has not been any specific review on SSIs applicable to PV systems. Hence the objective of this paper is to review some of the recent developments in the area of SSI. The first section of this paper talks about the introduction. Section two will explain the evolution of the architecture of grid connected PV inverters. As a boost converter is required to raise the voltage levels the third section will briefly talk about DC-DC converters. In section four some of the recent SSI topologies will be reviewed. The three most fundamental MPPT techniques (hill climbing, perturb & observe and incremental conductance) will be discussed in section five. The last section of this paper is a conclusion mentioned in section six.

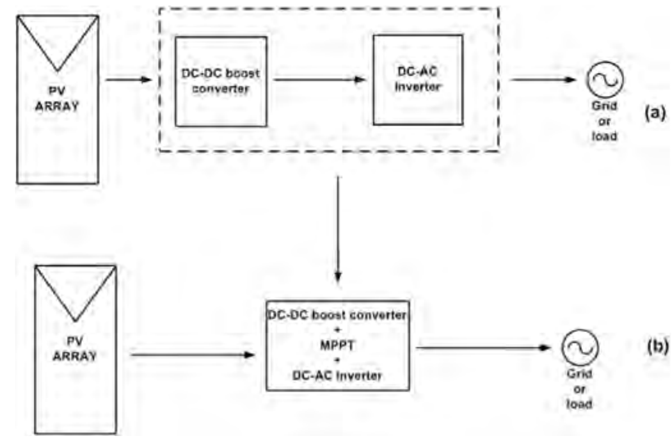

Fig. 2. PV based inverter (a) classical inverter with two stages (b) single stage inverter.

2. Evolution of grid connected PV inverters and various standards

The classical topologies used for the conversion of sunlight to AC and integration to the grid are the central inverters, string inverters, multi-string inverters, and the module inverters. The AC output could be either single-phase or three-phase.

2.1. Central inverters

The early central inverters used inverter topologies which were employed in the motor drives industry. The initial grid-connected PV inverters used the line-commutation technique (Fig. 4) for the commutation of thyristors [18]. As the technology has advanced, so the thyristors have been replaced by advanced semiconductor switches such as MOSFETs or IGBTs etc. The present day central inverters use self-commutation (Figs. 5 and 6) to turn-off the switches [18,19]. Central inverters consist of PV arrays connected in series for a higher DC voltage and such strings may be connected in parallel with the help of string diodes (Fig. 7a) to increase the current rating of the overall PV array [20]. The power rating of these inverters is of the order of several kilowatts [18,21]. These inverters were efficient and inexpensive, however, they suffered from the drawbacks of poor power factor (power factor lied in the range of 0.6 and 0.7) and high content of harmonics in the output current [22]. This inverter concept has some further disadvantages such as the inverter being subjected to a high magnitude of DC voltage by the PV modules, poor efficiency due to a common maximum power point tracking for all the PV modules employed, mismatch losses arising due to the different physical characteristics of PV modules and string diodes used in the system.

2.2. String inverters

String inverters can be considered as a derivative of the central inverters, as only one string of PV module provides input to the inverter. Various such systems may be connected in parallel to a common AC bus (Fig. 10b)). Any of the Figs. 4–7 and 8 [18,19,22–24] can be

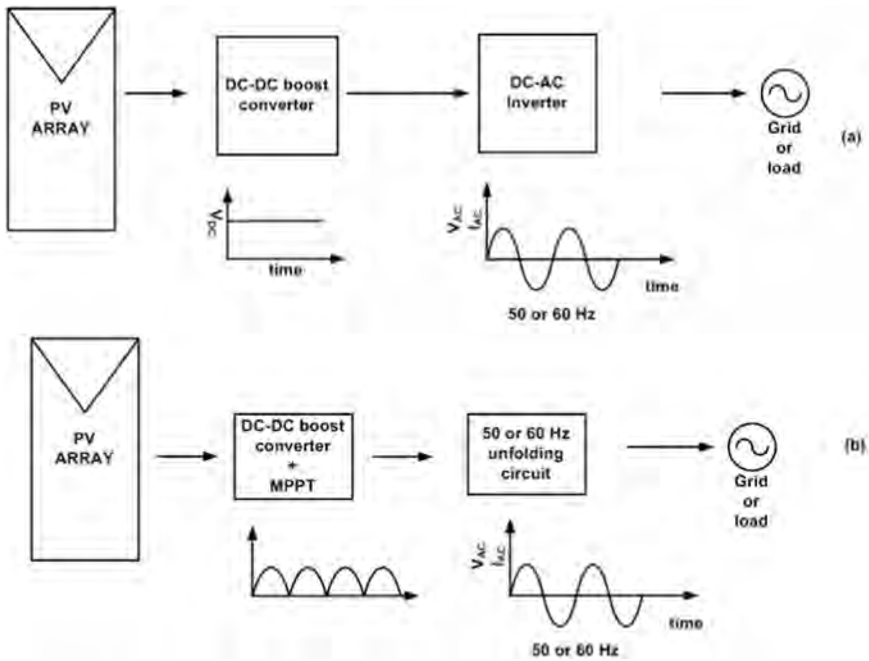

Fig. 3. PV based inverter (a) classical inverter with two stages (b) single stage inverter [7].

used to develop a string inverter [18]. The DC output of the PV string is quite high which avoids the need of voltage amplification. However if less number of PV modules are to be used then the options of using a DC-DC boost converter or a line frequency transformer for voltage amplification do exist. The advantages of string configuration include minimum losses, higher power output and increased reliability [20], the efficiency of string inverters is 1–3% higher than the central inverters [25] lying in a range of 94 to beyond 97% [19].

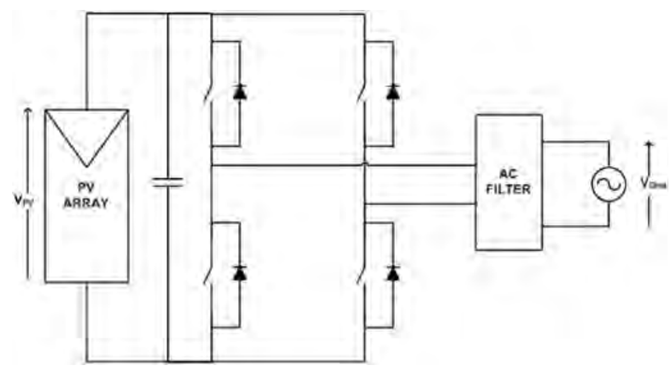

Fig. 5. Transformer less self-commutated PV inverter [19].

2.3. Multi string inverters

Multi string inverters (Fig. 10c) and (Fig. 9) [19,20,26,28] can be considered as a hybrid of string and central inverters as they combine the higher power output advantage of a string inverter with the economical cost of a central inverter. Several PV strings are connected to individual DC-DC converters [23,24]. All the PV strings employ individual MPPTs, extracting maximum power independently from each string. The output of all the DC-DC converters is connected to a common DC bus, which in turn is fed as an input to a common inverter. The AC output of this common inverter is then fed to the grid. Multi string inverters are flexible in nature as their power rating can be increased by connecting a PV string along with a DC-DC converter into the already existing system. This system is unreliable due to a common inverter. If a fault occurs in the inverter then the entire system goes down.

2.4. Module inverters

Due to the earlier mentioned disadvantages of the central inverters a different type of structure came into existence. This configuration was named as module inverter (Fig. 10d)) [20]. Module inverters are also

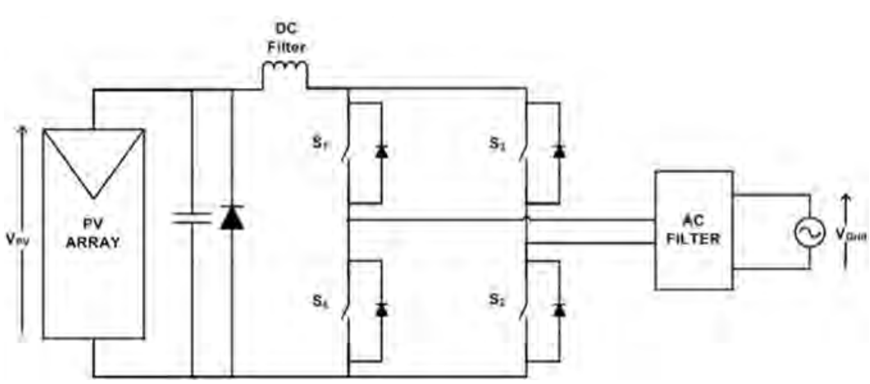

Fig. 4. Line commutated PV inverters [18].

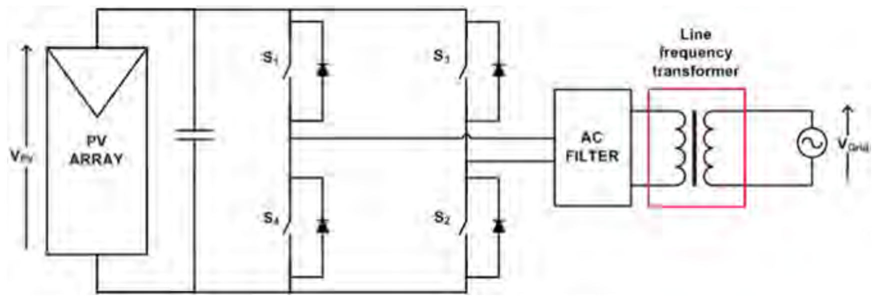

Fig. 6. A self-commutated PV inverter with line frequency transformer [19].

called module oriented inverters. Some of the advantages of this configuration are: use of similar components results in reduced costs and improved reliabilityeasier fault detection.

These are of the rating of up to 500 W [18]. Module inverters consist of one PV module connected to an inverter. Figs. 6 and 7 can be used to build a module inverter [19]. These inverters use self-commutation to turn-off the switches [27]. Structure wise, this is the smallest possible configuration. Use of only one PV module results in the elimination of mismatching losses. This configuration can be used as a plug and play device very easily. However as the power output of module inverters is very low they suffer from the disadvantage of poor efficiency. Also as the DC output of a single PV module is low, this DC has to be amplified to the required level with a higher value of amplification factor (Table 1).

2.5. Global PV inverter standards

The grid connected PV inverters have gained a lot of interest because of a continuous growth rate of 20–25% per annum over the last few years in the solar industry [29]. As these inverters can be connected to the grid, for reliable and safe operation and to ensure power quality these inverters must obey certain standards set by the electricity companies. There are several standards available in the market, like the International Electrotechnical Commission (IEC), Institute of Electrical and Electronics Engineers (IEEE), and National Electrical Code (NEC), which deal with the interfacing of PV inverters with the grid. Some of the widely used standards are IEC 61727 [30], IEEE 1547 [31], EN 6100-3-2 [32], IEEE 929-2000 [33]. Some of the standards specified by MNRE (India) [34] are IEC 62116, UL 1741, IEEE 1547. These standards apart from addressing grounding issues; specify the limits for voltage fluctuations in inverters, frequency variation range, operating power factor, current harmonics fed to the grid, DC current fed to the grid. These standards also deal with the detection of islanding operation. During Islanding phenomenon, the electrical connection between the inverter and the grid ceases to exist and the inverter continues to supply power to the local load if any. This disconnection could be intentional, or unintentional (accident or damage etc.). IEEE 1547 has been briefed in Table 2. A few more standards mentioned by MNRE (India) include IEC 62109-1 and IEC 62109-2 which together talk about the safety of power converters used in PV applications, IEC 61683 provides the procedure for efficiency measurement of PV systems under various loading conditions, IEC 62891 provides a method for measuring the accuracy of the maximum power point tracking of the inverters used for feeding grid, IEC 60255-27 is about measuring relays and protection apparatus, IEC 60068-2 (1, 2, 18, 27, 30 & 64) talks about the environmental testing of PV systems (inverters and power conditioners) and IEC 61000-2,3,5 focus on testing the PV inverters for electromagnetic interference (EMI) and electromagnetic compatibility (EMC).

3. DC-DC converters

From Figs. 2 and 3 [7] one can very well understand the importance a DC-DC boost converter plays in the design of an SSI. The conventional boost and buck boost converters can amplify the input voltage, however, those classic converters suffer from high switching losses and poor efficiency hence a need for high gain boost converters becomes obvious. In this section the authors shall only introduce some of the recent high gain boost converters and the gain summary of these converters has been presented in Table 3. An extensive review on DC-DC converters is present in [35,36].

Hwu and Yau [37] have proposed a step up converter which provides two different types of gains for two different configurations using four switches. Das and Agarwal [38] have a step up converter which uses one couple inductor, one switch, one passive clamp network and an intermediate capacitor along with other regular components to achieve a high gain. Siwakoti and Blaabjerg [39] have a high gain converter using one coupled inductor and a single switch. Banaei and

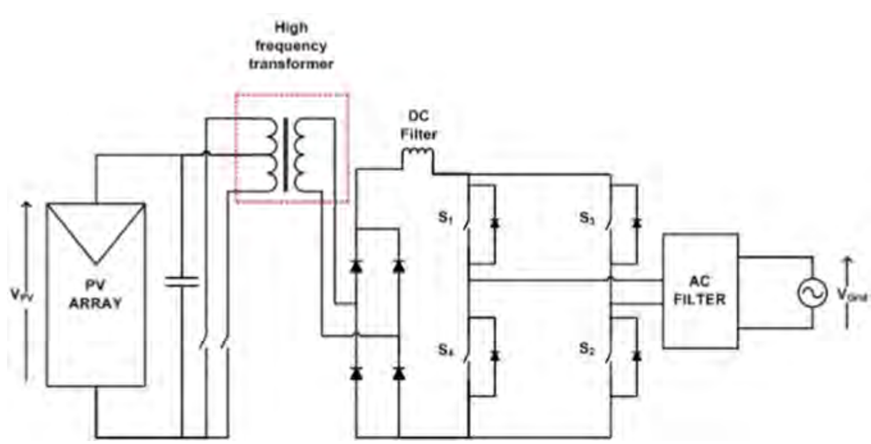

Fig. 7. PV inverter consisting of a high-frequency core based transformer [25].

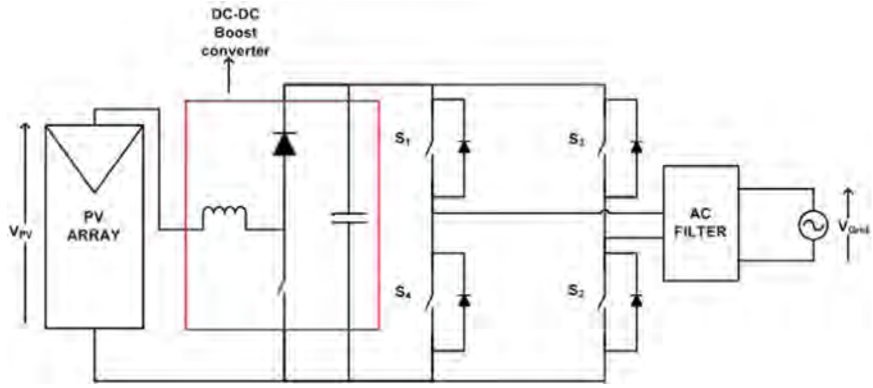

Fig. 8. A boost converter integrated grid connected PV inverter [23,24].

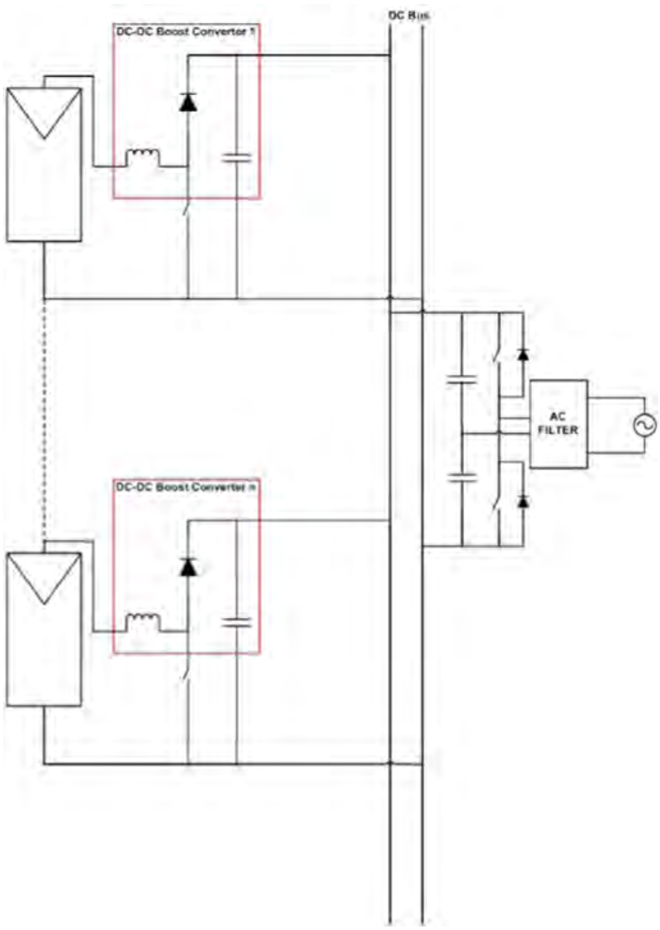

Fig. 9. A multi string inverter [26,28].

Bonab [40] have proposed a high gain step up DC-DC converter which requires a single and three individual inductors. Maheri et al. [41] have designed a step up converter a concept called active-passive inductor cells (APICs). In the formula, "n" is the number of APICs used in the circuit. Revathi and Prabhakar [42] have designed a step up converter which uses one three phase interleaved boost circuit, one coupled inductor and one voltage multiplier cell. Amirbande et al. [43] have designed a converter circuit which uses coupled inductors and switched capacitor concept to give high gain. Nag and Mishra [44] have proposed a converter circuit which uses two coupled inductors. Nouri et al. [45] have presented a ZVS based high gain DC-DC voltage converter. Ma et al. [46] have presented a boost converter which uses two switches and two coupled inductors. Feng et al. [47] have proposed a converter with two switches, three inductors, four capacitors and 5 diodes. Cao et al. [48] have proposed a design which uses two coupled inductors and two switches along with other components to achieve a gain higher than the conventional converters. A soft switched boost converter with high gain has been suggested by Sathyan et al. [49]. By integrating an interleaved boost converter with a voltage multiplier another high gain converter has been introduced by Baddipadiga and Ferdowsi [50]. A bi-directional converter which is non-isolated in nature and uses four switches has been suggested by Ardi et al. [51].

4. Single stage boost inverters (SSBI)

The advantages of SSIs have already been discussed in the introduction. The input of these SSIs can be connected to a PV array while their output can be connected to a grid or to an independent load like street lights or water pumps used for irrigation etc. Hence based on the kind of load they are connected to, these SSIs could be operated in two modes, namely, stand-alone mode or grid-connected mode.

By this paper a review of some (not all) of the recent SSIs would be done based on the mode of operation(buck, boost, buck-boost, flyback etc.), number of components employed, output of the inverter i.e. single phase or three phase etc.

4.1. Boost type SSI

Caceres and Barbi [52] have suggested a bi-directional boost converter based SSI (Fig. 11). The circuit consists of two bi-directional boost converters connected differentially across the load. Sliding mode control has been used to generate an AC output of 127 Vrms at a frequency of 60 Hz. The circuit is one of the earliest SSIs to have existed and has served as a prior art for many researchers. All the semiconductor components being switched ON and OFF at high frequency leads to switching losses and severe EMI concerns.

Zhou et al. [53] have proposed an SSI circuit based on coupled inductor (Fig. 12). An impedance network consisting a coupled network being fed by a DC source such as PV etc. is put before a classic three phase inverter bridge circuit to complete the overall circuit. P & O algorithm has been applied to extract maximum power from the input. Sine triangle PWM (STPWM) has been used to generate gate pulses. The circuit comprises a total of 3 stages namely the shoot through zero state, the open zero state and the active state. The primary side of the inductor is charged by the DC input whereas the secondary is charged by the capacitor C_1 during the shoot through state. The secondary winding charges till the point its voltage is higher than the voltage of C_1 after which the inductor feeds C_1 and during the same duration C_2 feeds L_1. During the open zero state all the upper switches together are in OFF state or all the lower switches. Secondary winding of the inductor along with L_1 charge up the capacitors C_1 and C_2 using the path offered by diode D_2. During the active state the coupled inductor as well as C_1

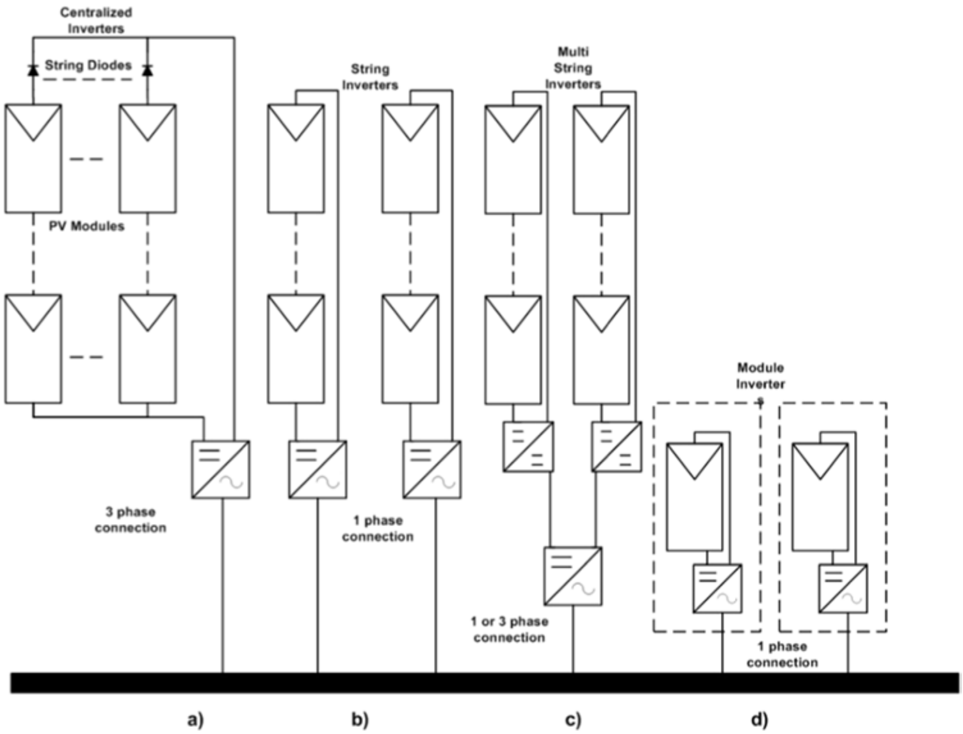

Fig. 10. The historical progression of grid connected PV inverters [20].

discharge through the load. During this state the current L_1 is zero and hence D_3 stays reverse biased. Furthermore the shoot through state duty ratio has been used as a control variable to stabilize the circuit. The researchers have tested their concept over a varied range of conditions, maximum output power being 783 VA, and meets the THD limit of 5% whenever the output power is 450 VA or above.

Zhou et al. [54] have proposed one more SSI which uses a tapped inductor (Fig. 13) to boost the input voltage. The circuit generates a three phase output and is suitable for stand-alone loads. The circuit draws continuous input current and ensures reduced voltage stresses across the two capacitors. Simple boost control is the strategy used to operate the circuit. SPWM technique has been employed to gate the semiconductor switches. For an electrical output between 480 W and 720 W the efficiencies are north of 91%.

A single stage grid connected inverter with inherent boosting ability has been introduced by Kan et al. [55] (Fig. 14). The circuit works in DCM and is capable of minimizing the low-frequency current ripple contained in the output current of a DC source such as a fuel cell by controlling the current through the boost inductor. The circuit consists of a boost converter which shares one of the inverter legs with itself. Switches S_1 and S_2 contain currents from the grid as well as the boost converter which results in higher current stress levels along with an increase in conduction loss.

An SSI with high gain has been proposed by Abramovitz et al. [56] (Fig. 15). The authors have used tapped inductor to increase the gain of their circuit. One cycle control (OCC) has been used to obtain an AC output of high quality. There are three states for each cycle of output. When the output is positive the first state lasts for a time duration of ta. During the first state switches M_1 and M_4 are ON along with diode D_2, while the switches M_3 and M_4 and diodes D_1 and D_3 are off. The input

Table 1
Summary of grid connected inverters [19–28].

Architecture type	Pros	Cons	Power rating
Central inverters	Low cost High power rating	Poor power factor Inverter is subjected to high voltage DC cables High harmonic contents in the output current Poor efficiency due to a common MPPT Mismatch losses	Several kilowatts to megawatts
String inverters	Reduced cost per watt Higher system efficiency Requirement of voltage amplification may be avoided No losses due to string diodes	Low power output as compared to central inverters If voltage amplification becomes necessary, the efficiency of the system comes down	Few kilowatts per string
Multi-string inverters	Local MPPT for each string Flexible system	Highly unreliable due to a common inverter	Few kilowatts
Module inverters	Reduced costs and improved reliability Maximum power is extracted from the PV module Least power loss No mismatch losses Easier fault detection Flexible system	Low power output High cost per watt Reduced efficiency Higher amplification factor Replacement is costly in case of inverter failure	Up to 500 W

Table 2
Requirements as per IEEE 1547 for interfacing PV inverters with grid [31].

Characteristics under observation	Limits as per IEEE 1547
Nominal power	30 kW
Maximum harmonic current distortion in percentage (Individual harmonic order h)	$(2 \le h < 11)$ 4.0% $(11 \le h < 17)$ 2.0% $(17 \le h < 23)$ 1.5% $(23 \le h < 35)$ 0.6% $(35 \le h)$ 0.3% Note: Even harmonics should be limited to 25% of the odd harmonic limits listed above.
Maximum current THD (total harmonic distortion)	5.0%
DC current injection	≤ 0.5% of the full-load output current
Voltage range for steady operation	88–110%
Frequency range for steady operation	59.3–60.3 Hz
Islanding	Inverter must detect the island and isolate itself from the grid within 2 s of formation of island

Table 3
Summary of latest high gain DC-DC converters [37–51].

Author(s)	Gain
Hwu and Yau [37]	$1 + 2D$; $2 + D$
Das and Agarwal [38]	$\frac{1+n}{1-D}$
Siwakoti and Blaabjerg [39]	$\frac{1+N}{1-D} + m$
Banaei and Bonab [40]	$\frac{3D}{1-D}$
Maheri et al. [41]	$\frac{1+(n+1)D}{1-D}$
Revathi and Prabhakar [42]	$\frac{3}{1-D}$
Amirbande et al. [43]	$\frac{1+N(1+D)}{1-D}$
Nag and Mishra [44]	$\frac{1+nD}{1-(2+n)D}$
Nouri et al. [45]	$\frac{1+6n}{(1-D)\left[1+\frac{72N^2Lk1fs}{Ro(1-D)^2}\right]}$
Ma et al. [46]	$\frac{2N+1+D}{1-D}$
Feng et al. [47]	$\frac{3+D}{(1-D)^2}$
Cao et al. [48]	$\frac{3+D+2n}{1-D}$
Sathyan et al. [49]	$\frac{1+2N}{1-D}$
Baddipadiga and Ferdowsi [50]	$\frac{4}{(1-d)}$
Ardi et al. [51]	$\frac{1}{(1-d)^2}$

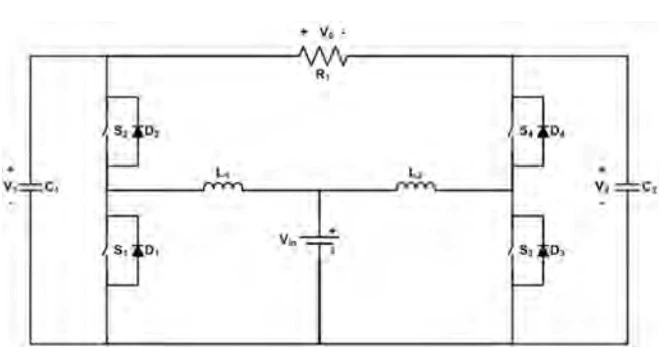

Fig. 11. A differential boost converter [52].

voltage source (V_g) charges the primary magnetizing inductance while the DC voltage (V_{DC}) appears across the input terminals of the output filter. Filter inductor (L_o) feeds both the filter capacitor (C_o) and the load (R_L). The next state is the second state which lasts for t_b duration. Switch M_4 continues to conduct while M_1 is switched OFF and M_2 is switched ON. Diodes D_1 and D_2 conduct in this state while D_3 remains OFF. V_g continues to charge the primary magnetizing inductance however the input terminals of the filter circuit are shorted hence L_o freewheels through C_o and R_L. The final duration lasts for a time period t_c. Switches M_1 and M_3 are switched ON whereas M_2 and M_4 are switched OFF. During this state the diodes D_1 and D_2 remain OFF and D_3 conducts letting the primary magnetizing inductance discharge itself through both the windings and in the process charges up the dc link capacitor (C_{dc}). L_o continues to freewheel through C_o and R_L as the input terminals of the filter circuit remain shorted in this state too. A worthwhile point about the proposed idea is the point at which the dc link capacitor has been placed. When the DC input voltage is of a high magnitude the size of the capacitor reduces. However in this circuit the voltage stresses across all the switches and diodes are very high and could lead the circuit to maloperation and make circuit less reliable with time by changing the physical parameters of these semiconductor devices [57].

Peter and Agarwal [58] have developed a SSBI based on the switched capacitor (SC) topology (Fig. 16). Their circuit can be used in stand-alone mode however with a slight modification the circuit has a scope to be connected in the grid-connected mode as well. The circuit designed by them employs several identical switched capacitor blocks being controlled with the help of rectified sinusoidal pulse width modulation (RSPWM). This circuit also consists of an output capacitor (C_o) which is load dependent. The DC input is 60 V with an AC output of 110 V at a frequency of 50 Hz. The circuit has an inversion efficiency of more than 95% and the THD is less than 4%. Perturb and Observance (P&O) has been used to track the maximum power and a tracking efficiency greater than 97% has been reported. The circuit provides an output which is almost twice the value of input however they have used 4 switched capacitor blocks taking the total switch count to 20 which makes this circuit costly, and the size and weight of the circuit also do increase as compared to other circuits.

Table 4 summarizes all the boost based SSIs.

4.2. Buck boost SSI

Jain and Agarwal [59] have proposed a single stage buck boost inverter (SSBBI) (Fig. 17). This circuit works in DCM and uses hill climbing algorithm to implement MPPT. STPWM technique has been used to trigger the switches. During the positive cycle the switch SW_{p1} is gated at high frequency and SW_{p2} remains ON for the entire positive cycle. Similarly during the negative cycle SW_{n1} is gated at high frequency and SW_{n2} remains ON for the negative cycle. When SW_{p1} or SW_{n1} are ON the respective inductors store energy and when the switches are OFF the two inductors supply power to the grid. While the circuit works in a symmetric fashion during both the cycles, making the circuit work in DCM has its own disadvantages such as lower efficiency, increased stress on the inductors and limited gain. Further the DC link capacitor used in this concept has a high rating which increases the size of this circuit.

Patel and Agarwal [60] have come up with a doubly grounded SSI which is transformer less (Fig. 18). Grounding is required to reduce the effects due to lightning and voltage surges. The circuit works fine even during partially shaded conditions. Another point about this circuit is the sharing of inductor. The circuit uses only one inductor (to boost the input voltage) which is used during both the cycles of output (positive and negative). This sharing of inductor ensures symmetrical operation of this inverter while working in buck-boost mode. Due to the buck-boost nature of this circuit no one needs to worry about the DC input being greater than or less than the grid requirement and thus the circuit provides flexibility in operation even during partially shaded condition. Hill climbing algorithm has been used with the help of sensors (which sense the PV voltages and currents) to extract maximum power. STPWM has been chosen to generate gate pulses at a switching frequency of 10 kHz. The circuit has three modes during each cycle of

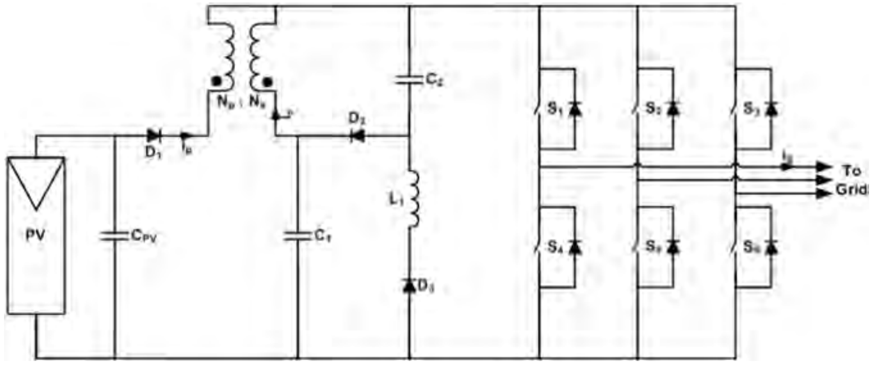

Fig. 12. A coupled inductor based SSI [53].

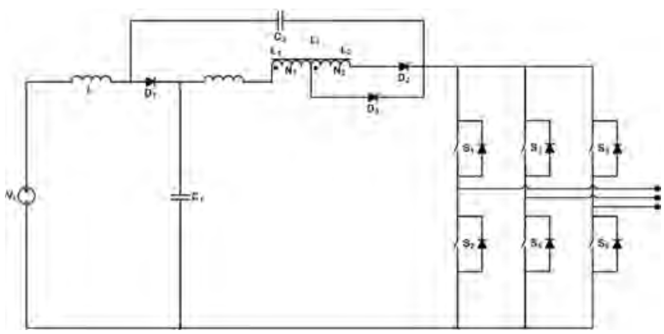

Fig. 13. A tapped inductor based SSI [54].

output. The inductor charges during the first mode and during the second mode this inductor provides input to the grid. During the third mode inductor current is zero and thus the circuit works in DCM. Even though the circuit works in a symmetrical manner i.e., buck-boost operation during both the cycles of output, a closer look into the operation reveals that the number of semiconductor devices working during a particular mode in both the cycles is different which results in unequal losses and unequal stresses during the two cycles. Another drawback of this circuit is the increased size and rating of the inductor as it is being shared in both the cycles.

Abdel-Rahim et al. [61] have replaced the inductors in [59] by SL topology to achieve a gain of sqrt (2) over the original configuration.

A buck-boost SSI (Fig. 19) to produce an AC output voltage of 230 V (rms) at 50 Hz to work in grid connected mode has been introduced by Petreus et al. [62]. The researchers have used hysteresis mode control technique to operate the circuit in a stable manner. The circuit has two stages of operation for every half cycle of the output voltage. During first stage of the positive cycle the inductor L charges through switches T_1 and T_2 whereas the switches T_3, T_4, T_5 and diodes D_1 and D_2 remain OFF. During the next stage the inductor L supplies the output through switches T_3 and T_5 and diodes D_1 and D_2. First stage of the negative cycle is exactly the same during the positive duration. The sequence changes however during the second stage of negative duration. The inductor L this time discharges and provides output through switches T_2 and T_4 and diode D_1. Hysteresis control allows the inductor current to vary between two extreme points however this variation in current results in low-frequency ripple current which can only be taken care of by a quality filter circuit. The filter circuit is in turn an increment in cost, volume and weight of this circuit.

Koushki et al. [63] have proposed a new topology in single-stage buck-boost inverters which is a modified version of the circuit suggested in [52] (Fig. 20). The proposed topology uses two buck-boost converters working every half-cycle with an auxiliary circuit comprising of an inductor in series with a capacitor, connected across the legs of the inverter. The output voltage is obtained by the control of duty cycles of both converters. Duty cycles along with the phase difference (φ) between legs, control the voltage appearing across auxiliary circuit (V_{aux}). Hence by controlling duty cycles, φ and Vaux the required output voltage (V_o) can be achieved. As the circuit employs ZVS for switching on and off the MOSFETs the switching losses are minimized resulting in an increased efficiency. With a DC input of 20 V the AC output for the proposed topology is 30 V.

Lo et al. [64] have developed an SSI (Fig. 21) which is bi-directional in nature. The circuit consists of several buck-boost converters connected in parallel on their output side and each of these converters is fed from an independent battery. The converter output is fed to a common dc-ac unfolder circuit. During the discharging mode this circuit feeds to the grid and works as a single stage buck-boost inverter. The circuit works in discontinuous conduction mode (DCM) while using RSPWM technique to trigger the switches. The circuit for an input of 50 V provides an AC output of 110 V at a frequency of 60 Hz with an efficiency of around 92%. Since a number of buck-boost converters are connected together hence a minimum of six switches, two diodes and one inductor are needed to realize this circuit.

Sreekanth et al. [65] have designed a SSBBI circuit (Fig. 22) using a high gain coupled inductor. The proposed circuit comes up with the advantages such as only one (Sp) of the five employed switches operates at high frequency resulting in less switching losses, use of coupled inductor brings with it a high gain, use of coupled inductor rather than two separate inductors results in the elimination of core requirement

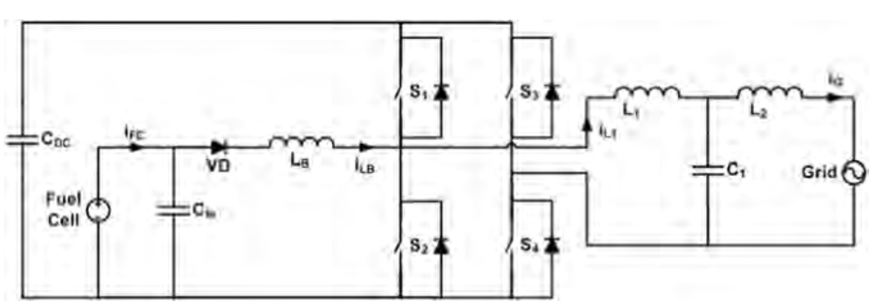

Fig. 14. A boost inverter with inherent boosting ability [55].

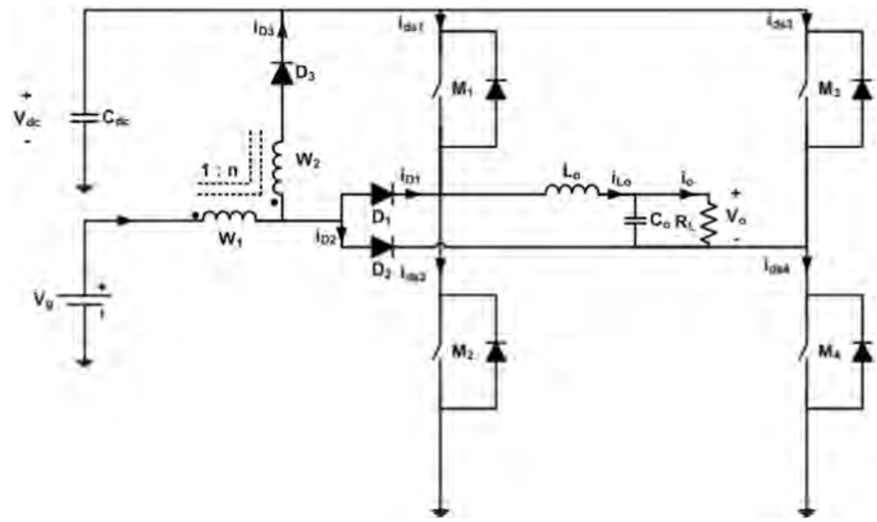

Fig. 15. A tapped inductor based SSI [56].

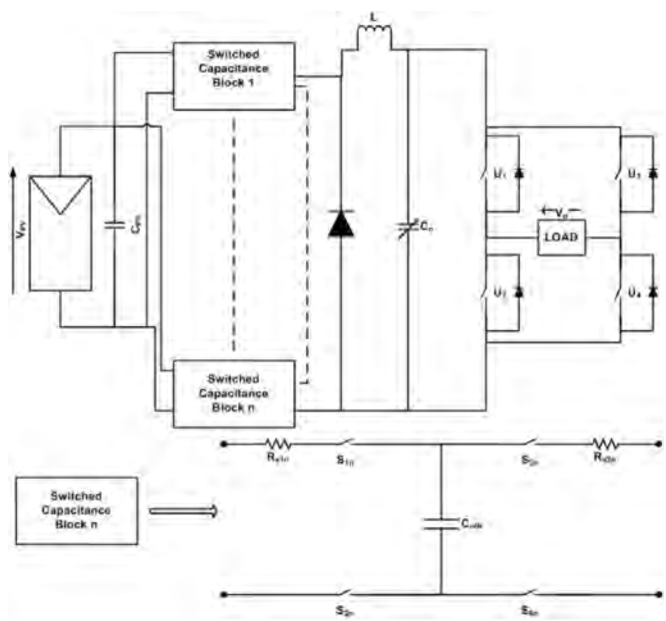

Fig. 16. SC based SSBI [58].

and reduced space. This circuit provides an AC output of 230 V at 50 Hz for a DC input of 60 V. The switch in series operates at a very high frequency however the remaining four switches operate at low frequency. Double loop control has been used to control the circuit and sinusoidal pulse width modulation (SPWM) has been used to generate the gate pulses. Efficiency provided by the authors is 86% for resistive load. THD values for resistive load is 3%, for R-L load it is 3.4% and for nonlinear load the value is 3.7%. Even though the gain of this circuit is pretty impressive due to high frequency switching this circuit can cause EMI.

Khan et al. [66] have developed a quasi-single stage buck-boost inverter (Fig. 23) which is capable of solving the current shoot-through issue and avoid the dead time due to pulse width modulation (PWM). The circuit uses MOSFETs resulting in high switching frequency and high efficiency. The proposed topology has the flexibility to be operated either in step-down or step-up mode. The peak efficiency of this circuit is 97.8% for a power output of 1.1 kW with a switching frequency of 30 kHz. This circuit can be used only in stand-alone mode. The input voltage range is 185–400 V DC with the output being 220 V AC at a frequency of 60 Hz.

The circuit proposed by Kumar and Sensarma [67] (Fig. 24) which eliminates common mode leakage current thereby protecting the PV panel from degradation and increasing its lifetime, is a single-stage buck-boost inverter consisting of 4 switches, 2 inductors and 3 capacitors one of which being a power decoupling capacitor (C_{in}) with an electrical power output of 300 W at 110 V and 50 Hz. The maximum efficiency of this circuit is 95.70% at rated load with an input of 100 V. The input range of this circuit is 60–100 V DC. They have used a multi loop control strategy, with the inner loop being controlled by a current programmed mode controller. The reference value for inner loop current is decided by an outer voltage loop. This topology can be employed both in grid-connected mode as well as stand-alone mode with a THD of 4.3% in grid-connected mode and 2.7%. 3.6% and 4.1% for resistive loads, inductive loads and non-linear loads respectively. Even with THD values very well below IEEE-1547 limits this circuit has a very low AC output gain.

Table 5 summarizes the various buck boost types SSIs.

4.3. Flyback based SSI

Kasa and Iida [68] developed a circuit (Fig. 25) based on the flyback converter concept. The proposed topology consists of three switches along with two diodes and a transformer with a tapping at the middle of secondary winding. To prevent any electrical accident the transformer provides isolation between the PV array and grid. The power output of this circuit is 300 W with an efficiency of about 89% while working in DCM. P&O MPPT without any current sensor has been used in this circuit to extract maximum power from the PV module. The proposed idea works in grid connected mode with an output of 100 V at 60 Hz frequency.

A flyback converter based SSI (Fig. 26) has been introduced by Shimizu et al. [69]. The average life time of electrolytic capacitors depends on the surrounding temperature and hence under high temperatures especially during summers the life of such capacitors decreases resulting in system failure and unreliable operation. One can always use film capacitors however they are costly and bulky which adds to the weight and volume of the overall system. The suggested design however uses capacitors with small capacitance values and hence allowing the usage of film or ceramic which results in an increase in reliability and inverter lifetime. The proposed inverter uses an extra circuit for power pulsation decoupling. Power pulsation is a serious concern because it happens at twice the value of output frequency and results in current ripple of low frequency on DC side which affects the input sources such as batteries, fuel cells or PV modules etc. The small

Table 4
Boost type inverters.

Author(s)	Caceres and Barbi [52]	Zhou et al.* [53]	Zhou et al.* [54]	Kan et al. [55]	Abramovitz et al. [56]	Peter and Agarwal [58]
Figure(s)	11	12	13	14	15	16
Switches	4	6	6	4	4	20
Diodes	4	3	3	1	3	1
Inductors	2	2 (1 tapped inductor)	2 (1 tapped inductor)	3	2 (1 tapped inductor)	1
Capacitors	2	2	2	3	2	5
Switching technique	–	STPWM	SPWM	SPWM	PWM	RSPWM
Switching frequency	30 kHz	10 kHz	10 kHz	20 kHz	50 kHz	35 kHz
MPPT	–	P & O	–	–	–	P & O
Control technique	Sliding mode control	Constant boost control	Simple boost control	–	OCC	SPWM control
Symmetry	Yes	Yes	Yes	Yes	Yes	Yes
Remarks	Low THD, high switching losses and high EMI	High gain, low THD	Efficiency reduces as gain increases	Eliminates low-frequency ripple current, high current stresses through switches and medium EMI	High voltage gain, however high voltage stresses across and current stresses through the switches and diodes, high EMI	High inversion and MPPT tracking efficiency, high EMI

– Implies not available.
* Implies three phase output.

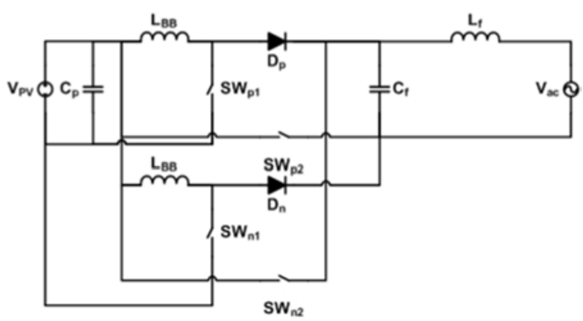

Fig. 17. SSBBI [59].

value film capacitors are connected across the DC input port and in the decoupling circuit. In all the entire circuit uses four switches, three diodes, three capacitors, one inductor and a high frequency transformer to convert the DC input into quality AC fed to the grid in DCM. A high switching frequency of 20 kHz allows reduction in the size of both the transformer core and the LC filter at the output. Low output current further ensures less conduction losses however the circuit suffers from high switching losses and EMI problem.

Another flyback converter based SSI has been proposed by Hu et al. [70]. An additional switch on the input side of the transformer has been added which isolates the decoupling capacitor from the PV panel. The circuit works in grid connected mode and the THD observed by the researchers was only 1.9%.

Chen et al. [71] have proposed a flyback based SSI (Fig. 27) which is a modification of the design proposed by Shimizu et al. [69]. The modified design includes an auxiliary circuit which performs two functions: 1) it decouples the input power pulsation, 2) it provides path to the leakage energy of transformer. The circuit uses a total of five switches, five diodes, two capacitors, one centre tapped transformer and one inductor, and feeds the grid working in DCM. This circuit works in four stages. During the first stage the primary winding of the transformer gets energized through D_1 and S_1 while the grid is fed by C_f and L_f. The second stage consists of two modes. All the switches and diodes except for D_{x1} and D_{x2} remain off during mode one. The grid is fed by C_f and L_f in stage two as well. The primary winding charges up the capacitor C_x when mode one is ON. During mode two S_{x1} and S_{x2} are switched ON and capacitor C_x feeds the primary winding through the path provided by S_{x1} and S_{x2}. It is during the third stage that the secondary winding feeds the grid. Polarity of the grid decides which devices conduct, S_2 and D_2 conduct if the grid voltage is in its positive cycle and during the negative cycle of grid voltage S_3 and D_3 conduct. During the final stage i.e. the fourth stage there is no current in either of

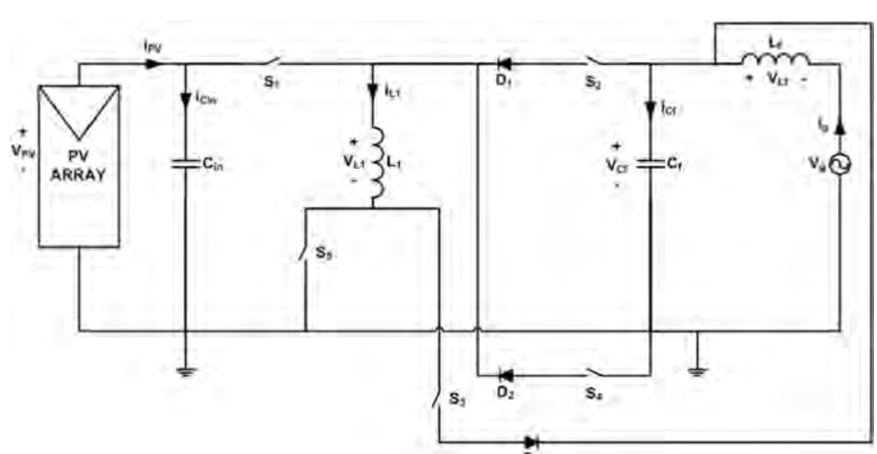

Fig. 18. Doubly grounded SSI [60].

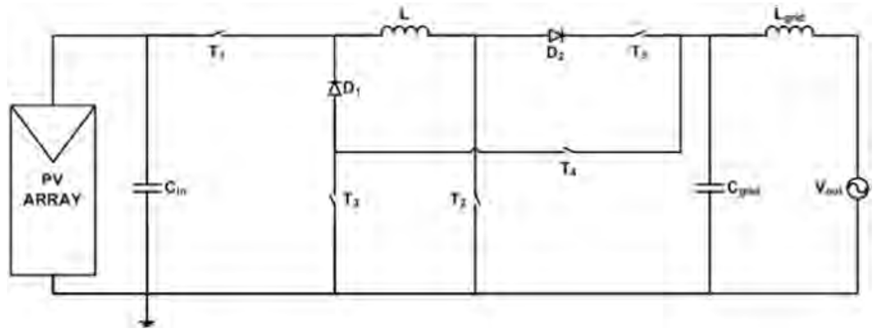

Fig. 19. A hysteresis mode control based SSBBI [62].

the two secondary windings and the grid is again fed by L_f and C_f and thus the circuit works in DCM. The authors have employed MPPT algorithm in their work however in the reviewed literature nothing has been mentioned about the type of MPPT algorithm used. While the circuit ensures no power pulsation exists and availability of galvanic isolation yet such a large number of part count and presence of transformer makes the circuit costly. Further it can also be noticed that the switching frequency is quite high which leads to EMI and switching losses. High levels of voltage stress across the semiconductor devices is yet another drawback of the proposed inverter.

The topology proposed in Zeng et al. [72] is a three port SSI (Fig. 28) where in the first port is connected to a PV array and the second port is connected to a battery. Solar energy cannot be available all the time, thus this three port system becomes advantageous and the battery can power the load in absence of sunlight. There is a bidirectional power flow in the second port. The battery gets charged during the availability of sunlight and feeds the load in its absence. In order to minimize the switching losses the authors have used ZVS to turn-on the switches. The proposed inverter is based on the flyback converter concept and uses the P&O algorithm for MPPT.

Abdel-Rahim et al. [73] have proposed a modified version of the circuit proposed by Kasa and Iida [68] wherein the flyback converter is followed by an unfolding circuit along with an L filter and works in DCM. The proposed configuration works in grid-connected mode and supplies sinusoidal current into the grid without measuring the output current. The transformer used in the flyback converter provides a galvanic isolation between the PV array and grid. RSPWM has been used to trigger the switch used in the flyback converter. This topology uses incremental conductance (IC) algorithm for MPPT.

All the flyback derived inverters have been put together in Table 6

4.4. Universal SSI

A universal SSI suitable for supplying the electric grid mode has been proposed by Prasad et al. [74] which is capable of performing all the three possible type of operations (Fig. 29) i.e. buck, boost and buck-boost under different switching patterns. The proposed concept works in DCM mode for the circuit to change its mode of operation (to change from any one of the three modes to either of the remaining to modes e.g. from boost mode to buck mode etc.). This feature of choosing any of the three modes at a given instant of time makes this idea unique. To provide gate pulses to the switches the authors have used PWM technique wherein the reference waveform has been compared with a triangular waveform of high frequency. Each configuration has three stages per every positive or negative cycle of grid voltage namely inductor charging, inductor discharging and zero current interval. During the positive cycle of grid voltage in buck mode inductor (L) charges when switches S_1, S_2 and S_5 along with diode D_1 are ON and S_3, S_4 and D_2 are OFF. The inductor discharges when S_1, S_2 and D_2 are ON and S_3, S_4, S_5 and D_1 are OFF. During the zero current interval S_3, S_4, S_5, D_1 and D_2 are OFF and S_1 and S_2 can be in any state i.e. ON or OFF. To perform boost operation in positive cycle the inductor charges when S_1, S_3, S_5 and D_1 are ON and S_2, S_4 and D_2 are OFF. The inductor discharges when S_1, S_2, S_5 and D_1 are ON and S_3, S_4 and D_2 are OFF. Zero current interval in boost mode during positive cycle requires S_3, S_4, D_1 and D_2 to be OFF and S_1, S_2 and S_5 can be in any state. To perform buck-boost operation in positive cycle inductor is charged by S_1, S_3, S_5 and D_1 keeping S_2, S_4 and D_2 OFF. Inductor discharges when S_1, S_2 and D_2 are ON and S_3, S_4,

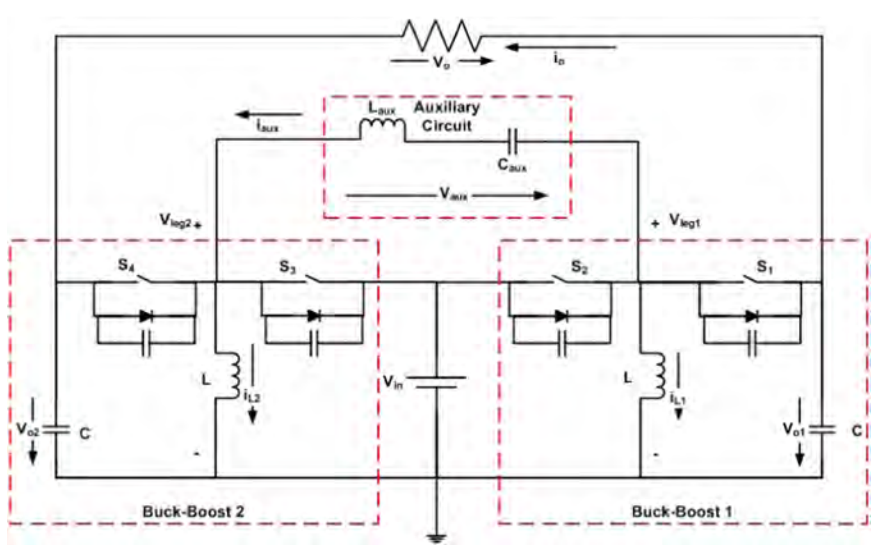

Fig. 20. A modified SSBI [63].

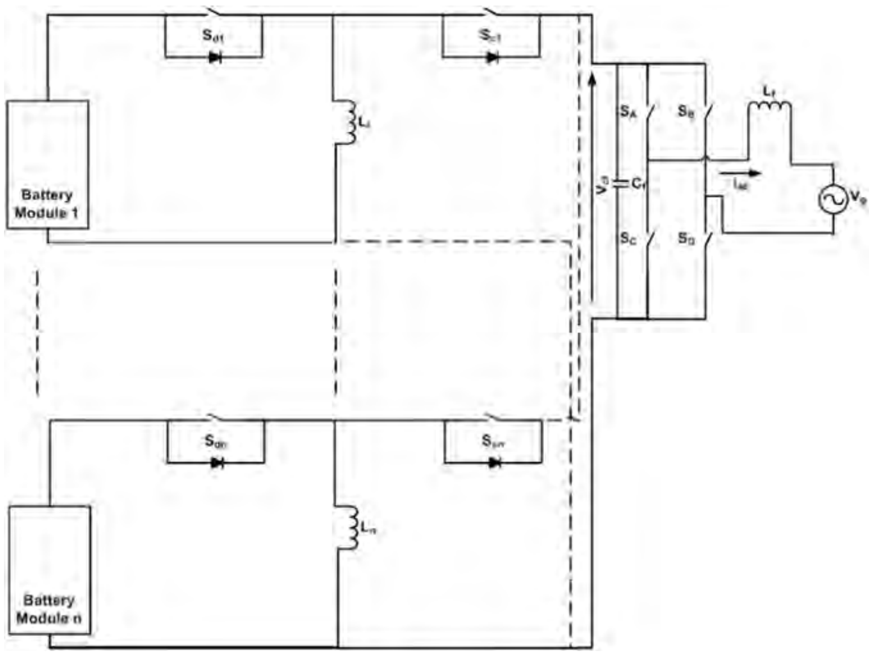

Fig. 21. A bi-directional SSI [64].

S_5 and D_1 are OFF. The zero interval in this case requires S_3, S_4, S_5, D_1 and D_2 to be OFF and is independent of the states of S_1 and S_2.

The concept used in [74] has been used by Lima et al. [75] with a slight modification that each switch is accompanied by a series diode. Another addition to the idea is that there are two inputs to the circuit wherein the first input is a PV source and the second input is a fuel cell (Fig. 30). The addition of fuel cell as input helps the circuit perform normally under abrupt weather changes. Even though the essence of both circuits [74,75] is exactly the same however the new idea works only in buck-boost mode. Both the input sources are connected to two different inductors (L_{PV} and L_{FC} respectively). The authors have used hysteresis control to control their idea with the output voltage and inductor currents as the control variables. P&O algorithm has been implemented to extract maximum power from PV. The efficiency of employed algorithm is around 99.8% with a tracking efficiency of 99.96%. For a THD of 3.9% the system efficiency was observed to be 78% and when the THD observed was 2.1% the system gave an efficiency of 86%. The results clearly show that decreasing THD would result in efficiency improvement.

Both the universal circuits are mentioned in Table 7

4.5. Cuk derived SSI

Pan et al. [76] have proposed a Cuk based SSI however with an added twist (Fig. 31). A flyback based auxiliary circuit has been combined with a Cuk based VSI in search of a higher voltage gain. The flyback circuit capacitors and the Cuk circuit capacitors charge in parallel while during discharging the capacitors from the two circuits discharge in series. This parallel charging and series discharging happens automatically. The voltage conversion ratio (GV) is given by the equation:

$$G_{V,proposed} = \frac{V_o}{V_s}\Big|_{proposed} = \left(\frac{1}{1-k}N_c + \frac{\alpha k}{1-k}N_f\right)M \tag{1}$$

where $\alpha = \frac{Lm}{Lk + Lm}$ is the coefficient of coupling of transformer T_f, k is the duty cycle of switch Q and M is the modulation index peak value. While the circuit provides high gain however it suffers from the drawbacks of being bulky, presence of the two transformers adds to the already existing conduction and switching losses, the efficiency of this idea decreases with increase in load and EMI concerns also exists for this circuit.

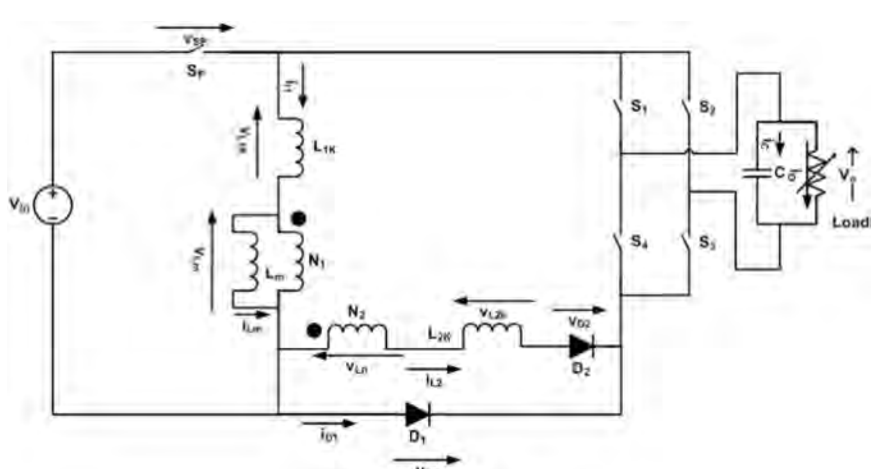

Fig. 22. A high gain coupled inductor based SSBBI [65].

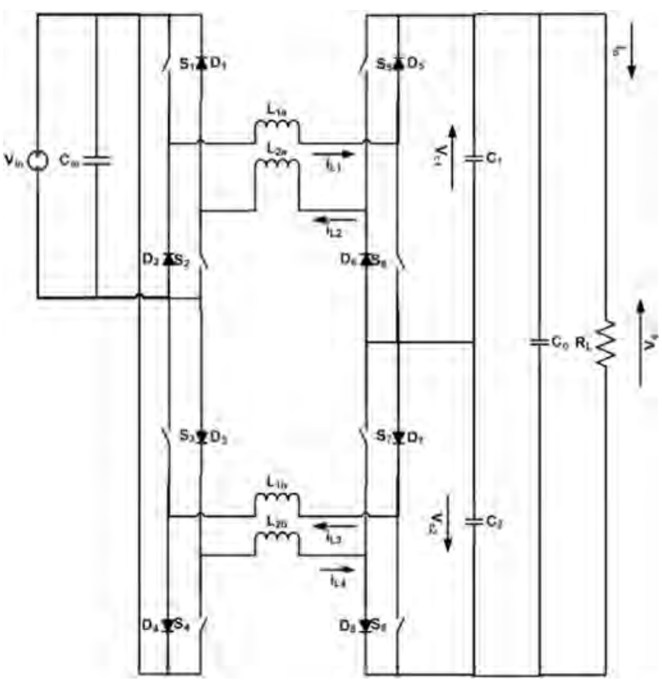

Fig. 23. A quasi SSBBI [66].

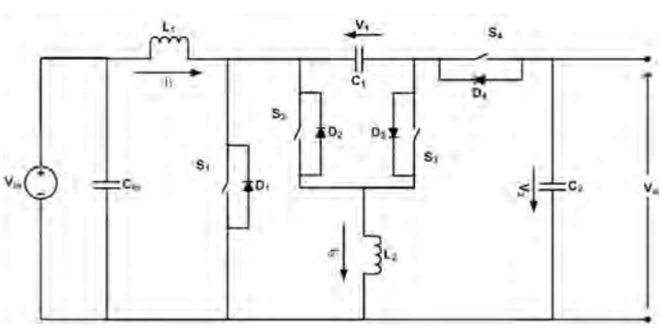

Fig. 24. A SSBBI capable of eliminating common mode leakage current [67].

Darwish et al. [77] have suggested a three phase differential SSI using Cuk converter. Connecting the converter output differentially across any load cancels the DC component present in the output voltage. Reduced size of energy storing components like capacitors and inductors provides better reliability and reduced size and cost of the circuit. The circuit works in both grid connected and stand alone mode.

Mehrnami and Mazumder [78] have come up with an inverter circuit, differential mode Cuk inverter (DMCI), based on the Cuk converter (Fig. 32). The output from the two converters is connected differentially across the terminals of a load. The circuit has two modulation schemes namely continuous modulation scheme (CMS) and discontinuous modulation scheme (DMS), the former initializes all the modules of this DMCI while the latter cuts off one module every half cycle of the output frequency. During CMS the DC voltage gain is linear for a longer duration and THD is also reduced. DMS brings down the circulating power and therefore losses are reduced, it also reduces the voltage ratings of the devices used. DMS requires a more complex closed loop compensation to limit THD to a satisfactory level. The circuit operates in a symmetrical manner during both the modulation schemes. The addition of two transformers makes the circuit bulky and adds to the overall cost. The transformers further contribute to the already existing conduction and switching losses in the circuit along with increased voltage stresses across the switches.

Gautam et al. [79] have proposed a single stage single phase inverter which is transformer less and has a common ground which

Table 5
Buck boost inverters.

Author(s)	Jain and Agarwal [59]	Patel and Agarwal [60]	Abdel-Rahim et al. [61]	Petreus et al. [62]	Koushki et al. [63]	Lo et al. [64]	Sreekanth et al. [65]	Khan et al. [66]	Kumar and Sensarma [67]
Figure(s)	17	18	–	19	20	21	22	23	24
Switches	4	5	4	5	4	At least 6	5	8	4
Diodes	2	3	8	2	0	At least 2	2	8	0
Inductors	3	2	5	2	2	At least 1	1	4	2
Capacitors	2	2	2	2	2	1	1	3	3
Switching technique	STPWM	STPWM	–	–	–	RSPWM	SPWM	PWM	PWM
Switching frequency	10 kHz	10 kHz	10 kHz	–	55 kHz	20 kHz	50 kHz	30 kHz	50 kHz
MPPT	Hill climbing	Hill climbing	IC	P & O	–	–	–	–	–
Control technique	–	–	–	Hysteresis control	–	RSPWM	Double loop	PWM control	Multiple loop
Symmetry	Yes	Yes	Yes	Yes	Yes	Yes	Yes	Yes	Yes
Remarks	Low gain, high current stresses on inductors	Resolves the challenges due to partial shading, unequal losses during the different output cycles, increased inductor size	High gain	High ripple content in inductor current	Employs ZVS switching technique to reduce switching losses, medium EMI	–	High gain, medium EMI	Eliminates dead time during PWM and solves current shoot through issue	Eliminates common mode leakage current, medium EMI

– Implies not available.

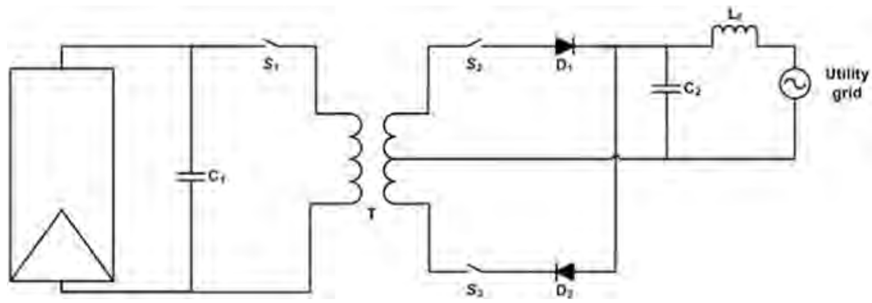

Fig. 25. A flyback converter based SSI [68].

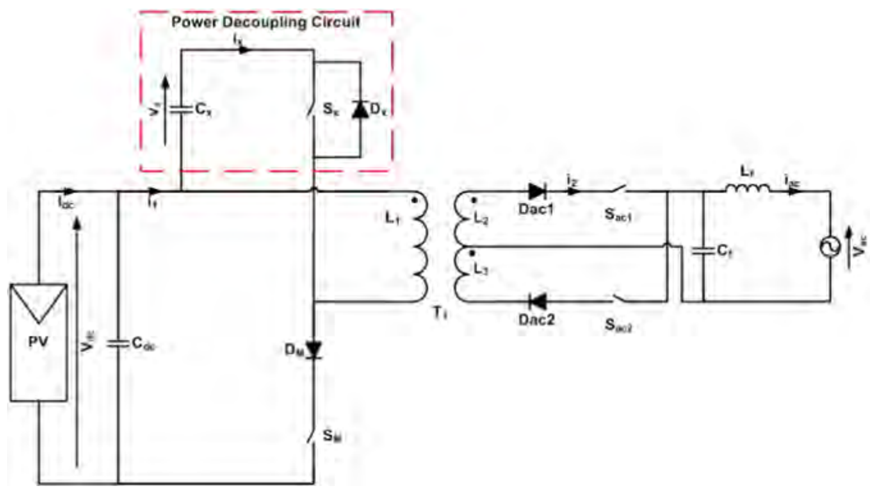

Fig. 26. A flyback back converter based SSI with power decoupling circuit [69].

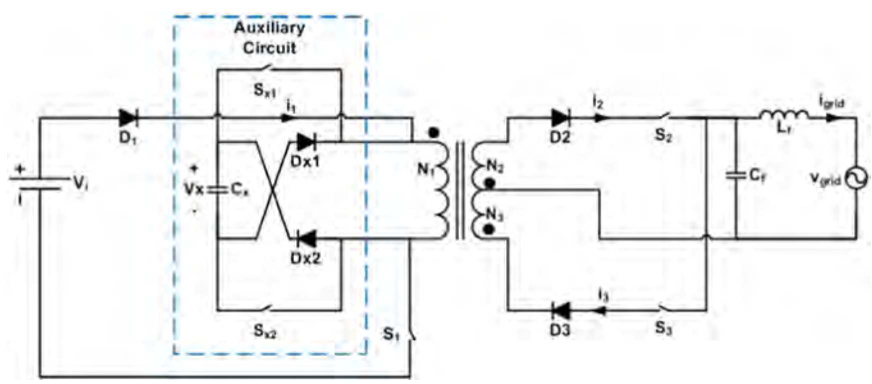

Fig. 27. A flyback converter with a modified power decoupling circuit [71].

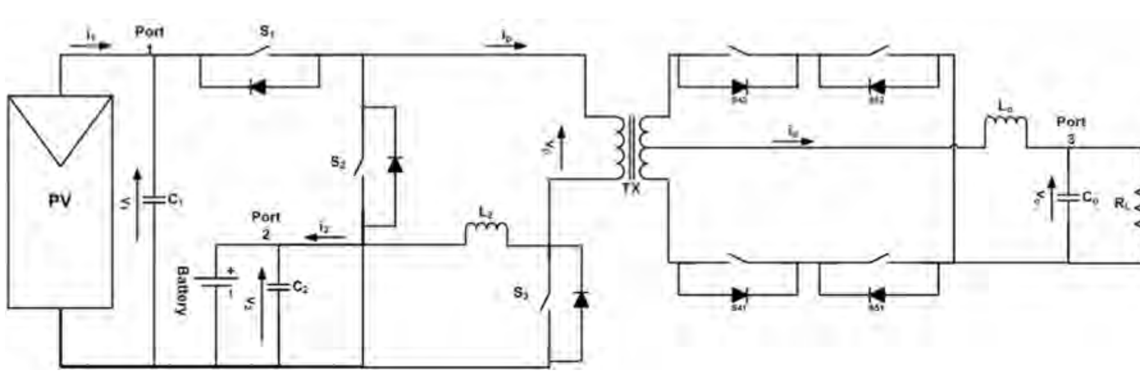

Fig. 28. A three power port flyback based SSI [72].

Table 6
Flyback based SSI.

Author(s)	Kasa and Iida [68]	Shimizu et al. [69]	Hu et al. [70]	Chen et al. [71]	Zeng et al. [72]	Abdel-Rahim et al. [73]
Figure(s)	25	26	–	27	28	–
Switches	3	4	4	5	7	5
Diodes	2	3	4	5	0	1
Inductors	1 centre tapped transformer	2 (1 centre tapped transformer)	2 (1 centre tapped transformer)	2 (1 centre tapped transformer)	3 (1 centre tapped transformer)	1 transformer
Capacitors	2	3	2	2	3	2
Switching technique	PWM	–	–	–	PWM	RSPWM
Switching frequency	9.6 kHz	20 kHz	50 kHz	50 kHz	200 kHz	–
MPPT	P&O	–	–	–	P&O	IC
Control technique	–	–	–	–	–	–
Symmetry	Yes	Yes	Yes	Yes	Yes	Yes
Remarks	Uses only three switches, isolates PV array from grid and no discharge current from PV to ground	Eliminates power pulsation, provides galvanic isolation, low efficiency, high switching losses and EMI problem	Provides galvanic isolation, high EMI and switching losses	Eliminates power pulsation, availability of galvanic isolation, large number of part count and transformer increases cost, high EMI and switching losses, high levels of voltage stress across semiconductors	Provides flexibility and reliability to the system, uses ZVS to minimize switching losses, very high EMI	–

– Implies not available.

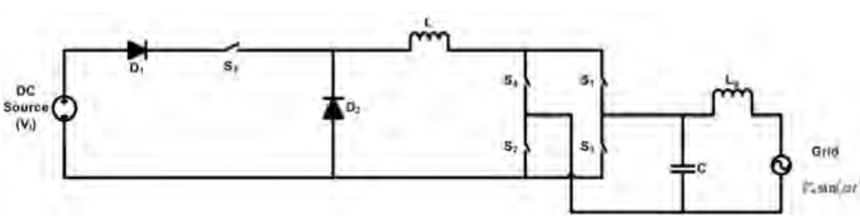

Fig. 29. A universal inverter [74].

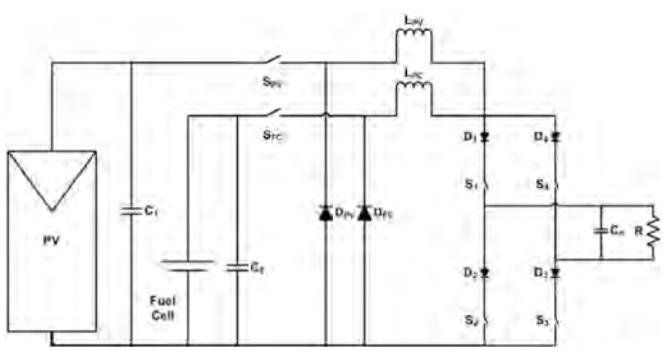

Fig. 30. A universal inverter with two DC inputs [75].

Table 7
Universal inverters.

Author(s)	Prasad et al. [74]	Lima et al. [75]
Figure(s)	29	30
Switches	5	6
Diodes	2	6
Inductors	2	2
Capacitors	1	3
Switching technique	PWM	–
Switching frequency	10 kHz	–
MPPT	–	P&O
Control technique	–	Hysteresis control
Symmetry	Yes	Yes
Remarks	Can perform all the three operations (buck, boost and buck-boost), uses DCM to decrease the size of L and C values	Provides flexibility and increases system reliability

– Implies not available.

eliminates the possibility of any common mode current between the input and the output. The proposed inverter is a combination of the Cuk and Watkins Johnson converters. Elimination of common mode current ensures increased PV lifetime. However the transfer function of output contains zeroes in right half plane (RHP) which results in a narrow closed loop bandwidth.

Chamarthi et al. [80] have come up with a design based on Cuk converter (Fig. 33) which can be used in grid connected mode. The salient feature of this circuit is that a common ground exists between the negative terminal of the PV array and the neutral point of the grid. This feature results in a low value of DC input voltage and also ensures that the value of leakage current passing through the parasitic capacitance of PV array is zero. The circuit uses six IGBTs wherein each IGBT is connected in series with a diode to block the flow of current in reverse direction, along with a PI controller to control the circuit. S_1, S_2, S_4 and S_6 operate at a frequency of 10 kHz while S_3 and S_5 operate at 50 Hz. The inductor connected on the PV side works in DCM. The DC side inductor reduces the ripple in input current and thus it reduces the size of capacitor placed across the PV terminals. However as there is no electrical isolation between the grid and PV safety becomes a major concern. The proposed prototype has a power output of 250 W with a theoretical efficiency of 95.5%.

All the Cuk converter based SSIs have been summarized in Table 8.

4.6. ZSI SSI

There are some limitations with the conventional voltage source inverters (VSI) and current source inverters (CSI). The classic VSI is in fact a buck or step down inverter. It has to be ensured that at no time both the switches from the same leg are gated. If such a situation

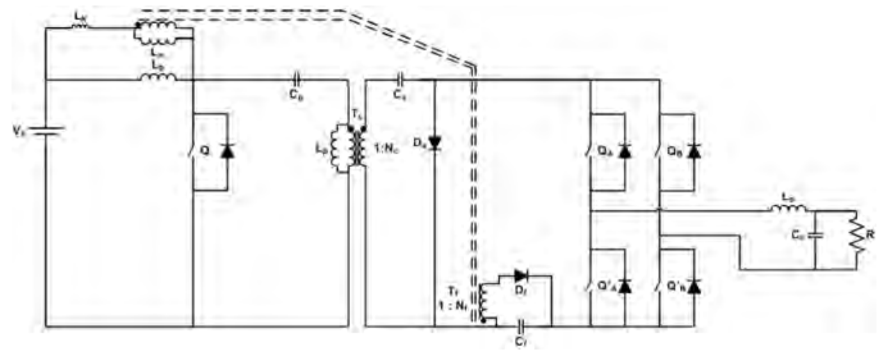

Fig. 31. A SSI based on the combination of a flyback and a Cuk converter [76].

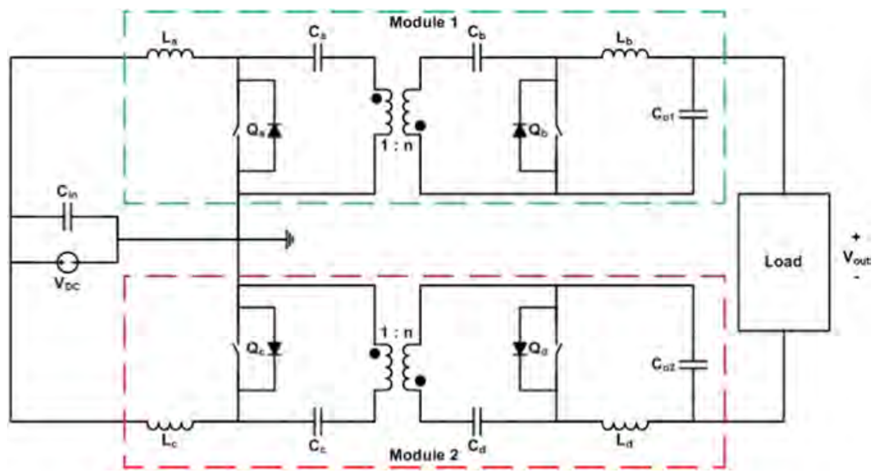

Fig. 32. A DMCI [78].

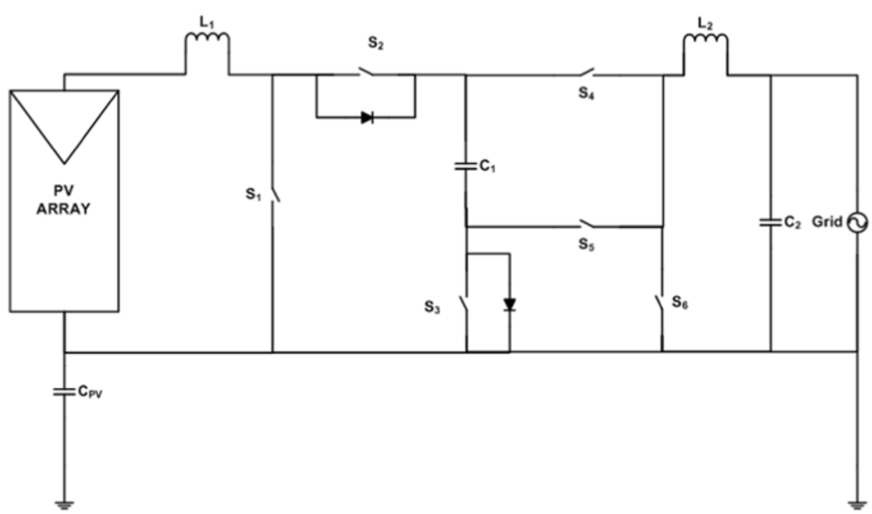

Fig. 33. A Cuk converter based grid connected SSI [80].

surfaces then it will result in a short circuit of the inverter circuit and currents with high amplitudes, capable of destroying the devices, will flow through the circuit. Also an LC filter at the output port is necessary to provide a sinusoidal voltage. While working with a CSI at least one of the upper switches and one of the lower switches should remain gated. If not ensured then an abrupt change in the flow of inductor current would lead to a voltage spike across the inductor capable of taking out the switches. To overcome these disadvantages Peng [81] has developed a single stage circuit (Fig. 34) called the impedance source inverter (ZSI) which offers a wide range of output voltage. The ZSI concept however suffers from the drawback that improper selection of inductor and capacitor values can lead to an unstable operation and the control of generating gate pulses will be an uphill task during such an instability.

Nguyen et al. [82] have suggested a design (called TZ- source inverter by the authors) (Fig. 35) based on the ZSI proposed by peng. The two inductors in the earlier circuit have been replaced by two transformers to increase the further. The boost factor of [81] is given by the equation:

Table 8
Cuk derived SSI.

Author(s)	Pan et al. [76]	Darwish et al.* [77]	Mehrnami and Mazumder [78]	Chamarthi et al. [80]
Figure(s)	31	–	32	33
Switches	5	6	4	6
Diodes	2	0	0	0
Inductors	3 (2 transformers)	6	6 (2 transformers)	2
Capacitors	4	–	7	2
Switching technique	–	–	–	SPWM
Switching frequency	40 kHz	50 kHz	125 kHz	10 kHz
MPPT	–	–	–	–
Control technique	–	–	–	–
Symmetry	Yes	Yes	Yes	Yes
Remarks	High gain, bulky, costly, low efficiency, high EMI	Reduced size of inductors and capacitors, high EMI and switching losses	Bulky and costly circuit, high voltage stress, high EMI	Common neutral between PV and grid, low DC input voltage, zero leakage current

– Implies not available.
* Implies three phase output.

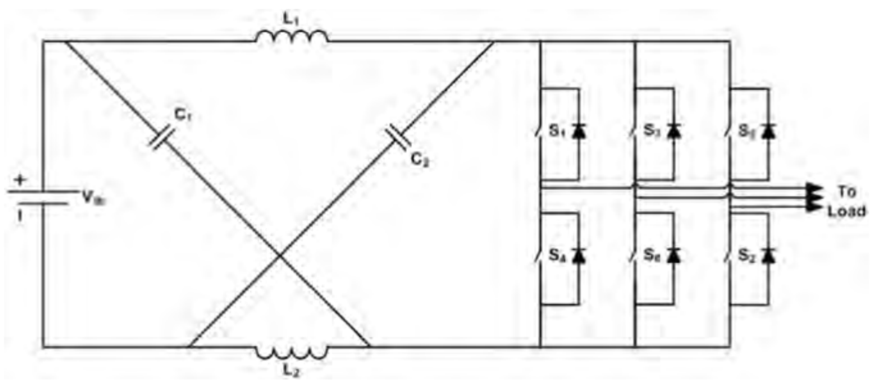

Fig. 34. A novel ZSI [81].

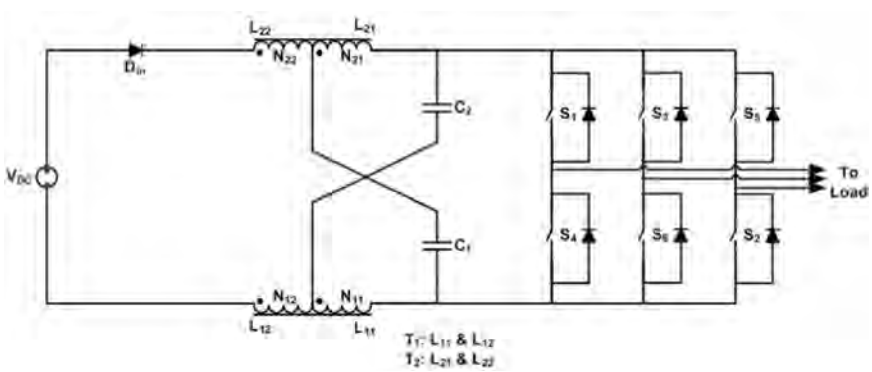

Fig. 35. A modified ZSI (TZSI) [82].

$$B = \frac{1}{1 - 2D} \tag{2}$$

Whereas the boost of the new circuit is given by the equation:

$$B = \frac{1}{1 - (1 + n)D} \tag{3}$$

where n is the turns ratio of the transformers used. This higher gain however has a flipside. Addition of transformers makes the circuit bulky and expensive and also the losses in the circuit increase along with increased voltage stresses on the switches.

The two ZSI concept based SSIs have been summarized in Table 9.

4.7. qZSI SSI

A three port qZS single stage three phase inverter (Fig. 36) has been proposed by Ge et al. [85]. The following equation has been used to control the power flow in the circuit:

$$P_{in} - P_{out} + P_b = 0 \tag{4}$$

P_{in} is the input power from PV, P_{out} is the power supplied by the inverter and P_b is the battery power. If P_{in} is less than P_{out}, P_b is greater than zero and i_{l2} is greater than i_{L1}, the battery discharges. If P_{in} is greater than P_{out}, P_b is negative and i_{L2} is less than i_{L1}, the battery charges. If P_{in} is equal to P_{out}, P_b is equal to zero and i_{L1} is equal to i_{L2}, there is no energy exchange in the battery. By working in CCM the current stress through the inductors reduces which further reduces the rating of the other components used.

Nguyen et al. [84] have proposed two SSIs (Figs. 37 and 38) both being qZSI. The conventional inductors have been substituted by the switched inductor (SL) concept. First idea is the ripple input current SLqZSI (rSLqZSI) and the second is continuous input current SLqZSI

Table 9
ZSI SSI.

Author(s)	Peng* [81]	Nguyen et al.* [82]
Figure(s)	34	35
Switches	6	6
Diodes	0	0
Inductors	2	2 transformers
Capacitors	2	2
Switching technique	PWM	–
Switching frequency	10 kHz	10 kHz
MPPT	–	–
Control technique	–	Simple boost control
Symmetry	Yes	Yes
Remarks	Improper selection of inductor and capacitor can result in unstable operation of the circuit	High gain, expensive, bulky, high losses and voltage stresses

– implies not available.
* Implies three phase output.

(cSLqZSI). Both the ideas are controlled using the simple boost control technique. The two ideas are capable of tackling the issues due to start up inrush current. The boost for rSLqZSI is given by the equation:

$$B_r = \frac{1 + D}{1 - 3D} \tag{5}$$

and the boost for cSLqZSI is given by:

$$B_c = \frac{1}{1 - 3D} \tag{6}$$

Using SL instead of a normal inductor provides higher gain but the part count of both the circuits increases along with the increase in size and weight.

Ho et al. [85] have come up with an active switch based quasi Z source inverter (ASqZSI) (Fig. 39) which promises lower levels of voltage stresses across the inverter switches, the circuit also promises of high voltage gain. The authors have tested their idea with a three phase Y-connected resistive load. The inductors charge during the shoot through state (when both the switches of the same leg of an inverter are ON the situation results in a shoot through) through switch S_7 and during this time the diodes D_1 and D_0 remain reverse biased. Constant boost control method has been used to control the circuit and to generate the gate pulses. A lower switching frequency of 5 kHz undoubtedly leads to lower value of switching losses however high values of inductor currents do result in higher conduction losses across the switches and diodes and can compensate for the reduced value of switching losses [86].

Table 10 summarizes the various qZSI based SSIs.

4.8. MCSI SSI

A multilevel current source inverter (MCSI) which uses only a single stage to extract the maximum power from input and invert the DC input to AC has been proposed by Cossutta et al. [87] (Fig. 40). This configuration works in grid connected mode taking the input from a fuel-cell and uses P&O algorithm to track the maximum power. Furthermore the circuit eliminates the necessity of the DC link capacitor which increases the life of the overall system as the mean time to failure is higher for inductors while compared to capacitors. The gating pulses have been generated using the phase shifted carrier SPWM (PSCSPWM) technique. Presence of the inductors on the input end ensures that the current fed by the input to the circuit has a low ripple current. One careful look at the literature reveals that because of the low DC output of the fuel cell a boost converter had to be used to raise the DC value to a sufficient level which would act as input to the MCSI. Even though this MCSI reduces THD and voltage stresses on the switches further drawbacks include higher component count which results in higher cost, higher conduction and switching losses and requires complex control methodology.

4.9. Zeta SSI

Surapaneni and Rathore [88] have proposed a zeta converter based SSI (Fig. 41) which works in continuous conduction mode (CCM). CCM leads to a circuit with higher efficiency, lower levels of current stress and lower rating of components. This idea based on zeta converter contains a high frequency centre tapped transformer to isolate input from output along with five switches, one inductor and three capacitors. One of the switches is on the DC side of the transformer while the remaining ones are connected on the load side. The DC side switch is operated on a high frequency while the load side semiconductor devices work on line frequency to feed an independent load. The circuit however suffers from the issues such as EMI and high levels of voltage stress on the load side switches.

4.10. SEPIC SSI

Kumar et al. [89] have also proposed a transformer less SSI which is doubly grounded. This inverter is based on the design of SEPIC

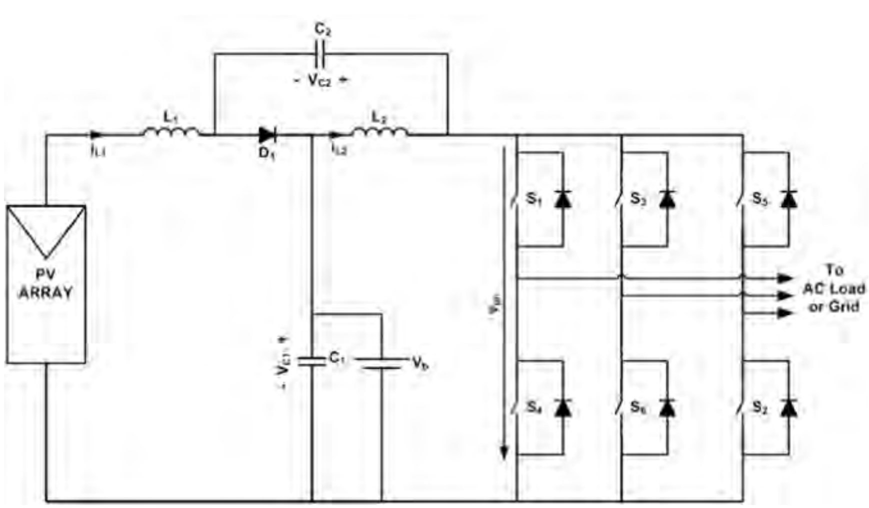

Fig. 36. A three port qZS-SSI [83].

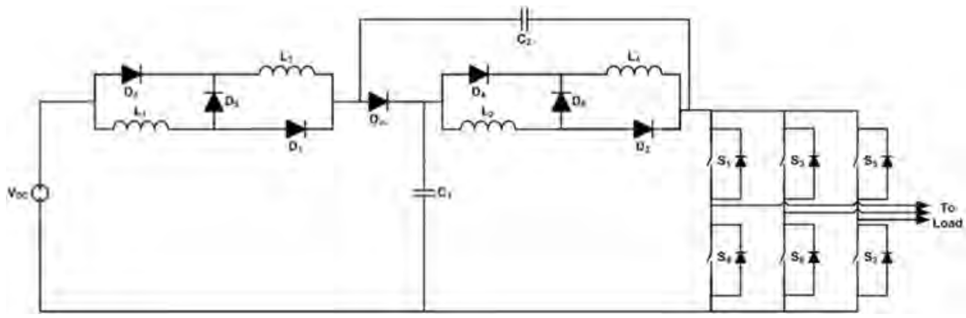

Fig. 37. A rSLqZSI [84].

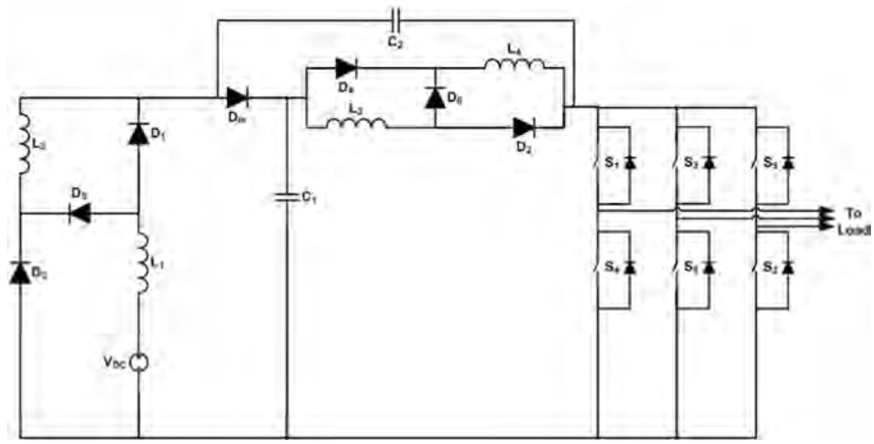

Fig. 38. A cSLqZSI [84].

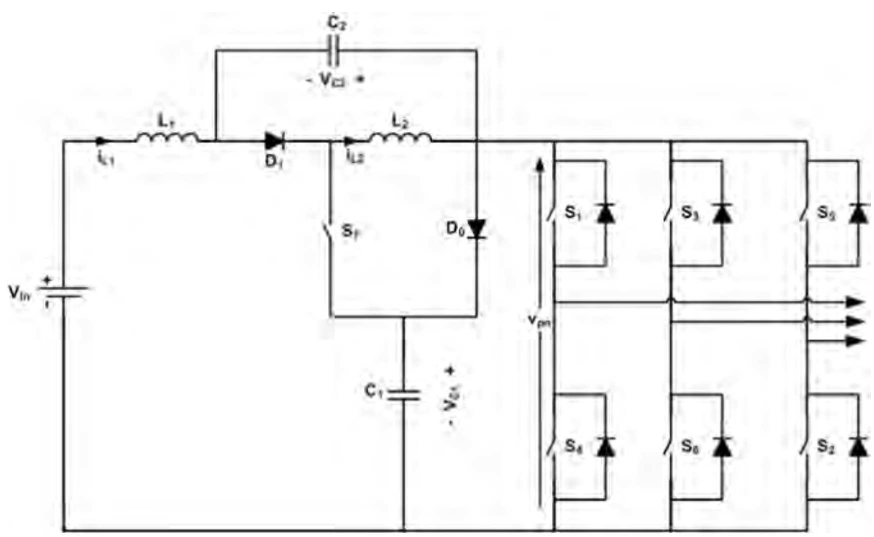

Fig. 39. An active switch based qZSI (ASqZSI) [85].

converter wherein the load side inductor has been replaced by a coupled inductor. SEPIC converter is a non-inverting buck-boost converter. The circuit consists of four switches, Coupled inductor leads to a higher gain compared as compared to a normal inductor. Double loop control loop has been used to control the circuit and a switching frequency of 50 kHz has been used for triggering the switches. Even though coupled inductor provides a higher gain but this advantage also leads to high stresses across the switches. Furthermore as the switching frequency is high EMI concern can't be overlooked either.

Table 11 summarizes MCSI, SEPIC and Zeta based SSIs.

Table 12 summarizes the advantages and disadvantages of the various topologies discussed from Sections 4.1–4.10.

5. MPPT

The basic principle of several MPPT approaches relies on the observation of variation in currents and voltages which occur because of pulsations in instantaneous power. Processing these changes lets anyone to find out the power gradient and lets that person decide if the PV system is working in vicinity of the maximum power point coordinates [90]. The maximum power supplied by a PV array is:

$$P_{\max} = V_{mpp} * I_{mpp} \tag{7}$$

Where $Vmpp$ and I_{mpp} correspond to the points of optimum performance i.e, maximum power. As the V-I characteristics of a PV array are

Table 10
qZSI SSI.

Author(s)	Ge et al.* [83]	Nguyen et al.^* [84]	Nguyen et al.^^* [84]	Ho et al.* [85]
Figure(s)	36	37	38	39
Switches	6	6	6	7
Diodes	1	7	7	2
Inductors	2	4	4	2
Capacitors	2	2	2	2
Switching technique	–	–	–	–
Switching frequency	–	10 kHz	10 kHz	5 kHz
MPPT	Hill climbing	–	–	–
Control technique	–	Simple boost control	Simple boost control	Constant boost control
Symmetry	Yes	Yes	Yes	Yes
Remarks	Provides flexibility of operation	High ripple in input current, high part count and bulky	high part count and bulky	High voltage gain, low switching losses, high conduction losses

– Implies not available.
^ Implies rSLqZSI.
^^ Implies cSLqZSI.
* Implies three phase output.

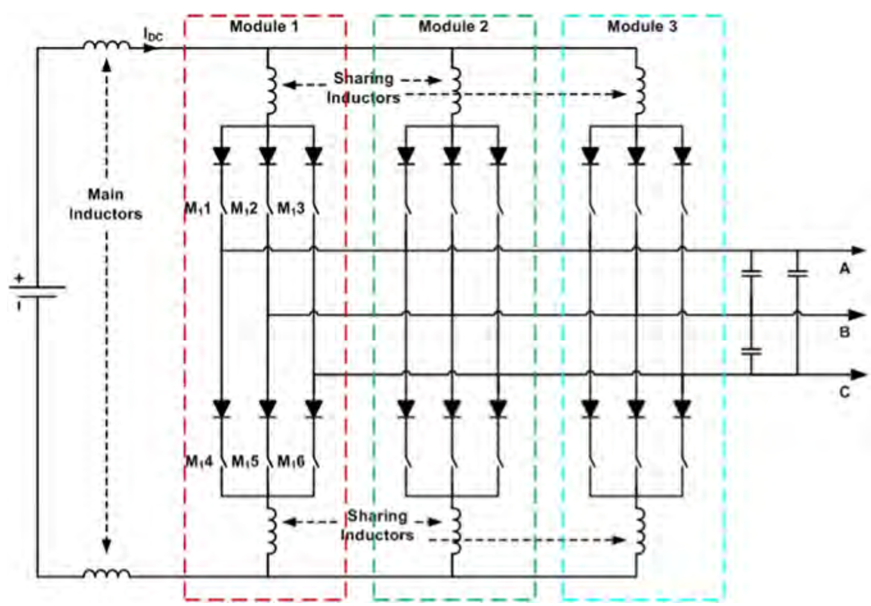

Fig. 40. Current source Inverter (MCSI) [87].

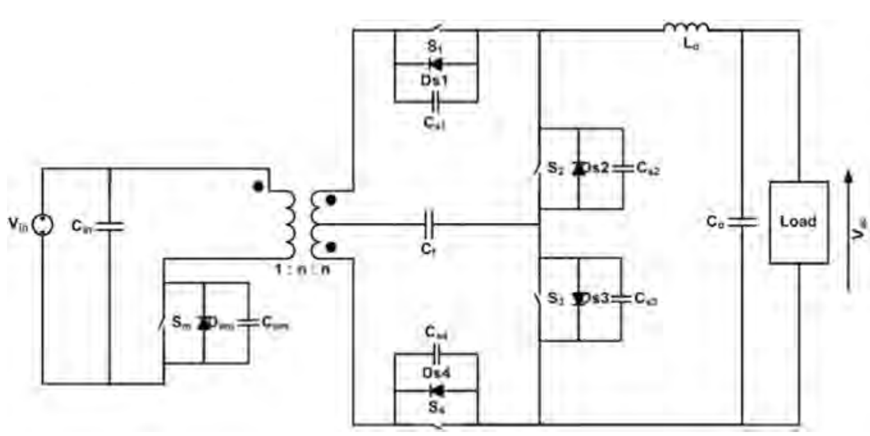

Fig. 41. Zeta converter based SSI [88].

nonlinear in nature, the need for an intelligent control becomes necessary which can trace the maximum power and can match the current with environmental changes [91]. MPPT is realized by varying the duty cycle of a power electronic circuit so that the load impedance, when reflected onto the PV side, becomes equal to the impedance value of PV. In this paper three of the most common approaches: hill climbing, perturb and observe and incremental conductance shall be explained. Rigorous and extensive reviews on different types of MPPTs are however available in [16,17].

Table 11
MCSI, Zeta and SEPIC inverters.

Author(s)	Cossutta et al.* [87]	Surapaneni and Rathore [88]	Kumar et al. [89]
Figure(s)	40	41	–
Circuit type	MCSI	Zeta	Sepic
Switches	18	5	4
Diodes	0	0	0
Inductors	8	2 (1 centre tapped transformer)	2 (1 coupled inductor)
Capacitors	0	3	3
Switching technique	PSCSPWM	–	–
Switching frequency	9.45 kHz	100 kHz	50 kHz
MPPT	P&O	–	–
Control technique	–	–	Double loop control
Symmetry	Yes	Yes	Yes
Remarks	Reduced THD and voltage stresses, high component count, high cost, high conduction and switching losses and requires complex control methodology	Low current stresses and low component ratings, EMI and high levels of voltage stress on the load side switches	High EMI

– Implies not available.
* Implies three phase output.

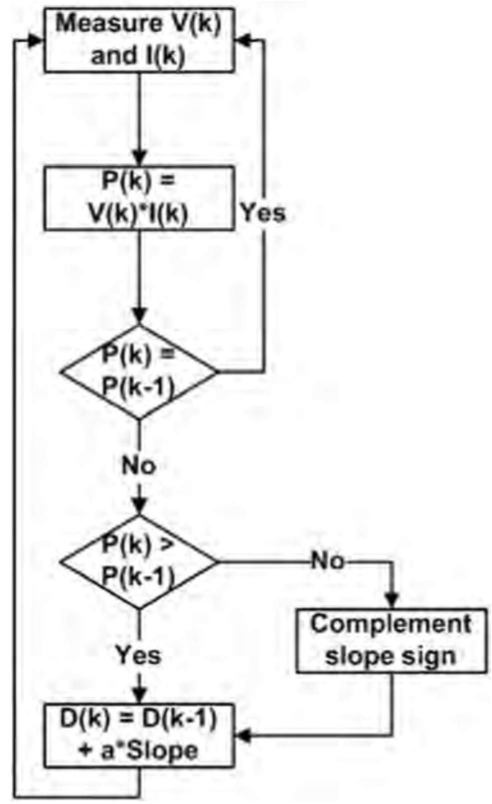

Fig. 42. Flow chart for hill climbing algorithm [93].

5.1. Hill climbing method

Hill climbing (HC) is one of the first approaches developed to track maximum power from PV. Because of its simplicity and ease of implementation this approach is used frequently [92–94]. To implement this algorithm PV voltage and current are measured using sensors and by multiplying the measured voltage with measured current the instantaneous output power is calculated and thus the duty cycle for a converter is varied appropriately to trace maximum power [93]. Fig. 42 presents the flow chart for HC MPPT [94] where "a" is the incremental duty cycle.

5.2. Perturb and observe method

Perturb and observe (P&O) is an easy to implement algorithm however it is not used for high power applications. Sensors measure voltage and current and thus the PV output is calculated after which voltage perturbations are brought to the circuit to determine the tracking direction. On the basis of these voltage perturbations the output power may rise or fall continuously. As the algorithm continuously monitors the point of maximum power using voltage perturbations and so the output power oscillates in the vicinity of MPP [95]. Fig. 43 shows the flow chart of a simple P&O algorithm [96].

5.3. Incremental conductance method

The slope of PV array power-voltage curve is zero at MPP. This fact is used in incremental conductance algorithm to track MPP. As the operating point moves towards the left of MPP the slope becomes

Table 12
Advantages and disadvantages of the various SSI topologies from Sections 4.1–4.10.

Topology	Advantage(s)	Disadvantage(s)
Boost [52–56,58]	High gain, low THD, low frequency ripple current elimination	High switching losses and EMI, reduced efficiency with increased gain, high voltage and current stresses
Buck-boost [59–67]	High gain, dead time during PWM eliminated, common mode leakage current removed	High current stress on inductors, increased inductor size, EMI
Flyback [68–73]	Availability of galvanic isolation, eliminate power pulsation,	Low efficiency due to transformer losses, increased cost, size and weight, high EMI
Universal [74,75]	Can perform all the three operations (buck, boost and buck-boost)	EMI
Cuk [76–78,80]	Continuous input and output currents, high gain	Bulky, costly, high voltage stress on switches, high EMI
ZSI [81,82]	High gain	Improper selection of inductors and capacitors can result in unstable operation of the circuit, expensive, high conduction losses and voltage stresses
qZSI [82–85]	High voltage gain, low switching losses	High ripple in input current, high part count, and bulky
MCSI [87]	Reduced THD and voltage stresses	High component count, high conduction and switching losses and requires complex control methodology
Zeta [88]	Low current stresses and low component ratings	High voltage stress on load side switches, EMI
SEPIC [89]	–	High EMI

* Implies three phase output.
– Implies not available.

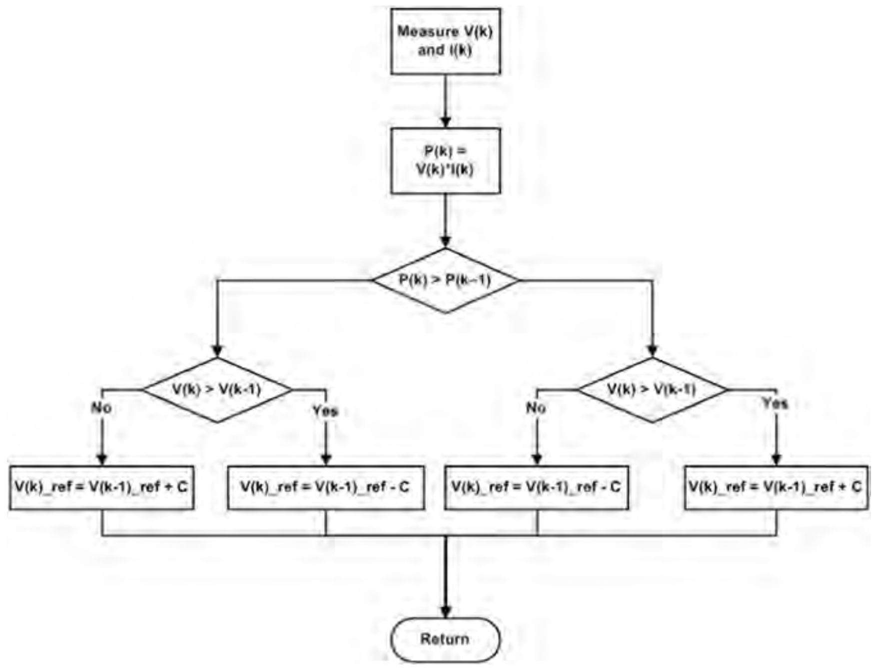

Fig. 43. Flowchart for P&O technique [96].

positive and when the operating point moves right of MPP value of slope becomes negative. Mathematically it can be written as:

$$dP/dV = \begin{cases} 0, & at\ MPP \\ >0, & left\ of\ MPP \\ <0, & right\ of\ MPP \end{cases} \tag{8}$$

$$\frac{dP}{dV} = \frac{d(IV)}{dV} = I + V\frac{dP}{dV} = I + V\frac{\Delta I}{\Delta V} \tag{9}$$

On comparing (7) and (8),

$$dP/dV = \begin{cases} -\frac{I}{V}, & at\ MPP \\ > -\frac{I}{V}, & left\ of\ MPP \\ < -\frac{I}{V}, & right\ of\ MPP \end{cases} \tag{10}$$

To track MPP ratio is taken between instantaneous conductance $\left(\frac{I}{V}\right)$ and incremental conductance $\left(\frac{\Delta I}{\Delta V}\right)$. Fig. 44 shows the flow chart for IC MPPT [97].

In this section the three most popular and most common MPPTs namely HC, P&O and IC were discussed.

6. Conclusion

A review of SSI was attempted in this paper. First stage discussed the advantages of solar energy and an idea about SSI was also given in the introduction itself. The second chapter was about the evolution of grid connected inverters and various quality standards being followed worldwide. Then a quick look on recent advances in step up converters was done in the third segment. The fourth segment extensively talked about some of the SSI existing in present time. It is up to the researchers which kind of topology they want to work with because each concept has its own advantages and disadvantages and to achieve one objective compromise has to be made with other things. Based on the review of SSIs done so far certain observations have been made which the authors would like to put in this segment. One can either go for a direct SSI with a high gain or the second option is to come up with a high gain DC-DC converter which employs MPPT and integrate this step up converter with an unfolding circuit. A high switching frequency leads to a reduction in the size of passive components such as inductors or capacitors but EMI concerns can't be overlooked when the circuit works at high frequencies. To avoid EMI switching frequency can be reduced but this would make the sizes of inductors and capacitors to grow bigger which will add to weight and cost of the circuit. And since there is nothing like an ideal inductor or an ideal capacitor, these components would add to the conduction losses. DCM operation leads to a high power factor operation however the inductor has to go through severe current stresses during DCM which asks for higher rating components. The efficiency of the circuit also goes down during DCM. The efficiency during CCM is higher as compared to efficiency during DCM, however CCM operation can result in core saturation of magnetic components which in itself is a huge drawback. Using a DC link capacitor in parallel with a DC source filters out power pulsation and peak to peak voltage ripples. The size of a DC link capacitor is inversely proportional to the applied DC voltage and the output ripple required [20]. Most of the circuits use electrolytic capacitors because of their cost and size however their life decreases during high-temperature operations making the circuit less reliable. Using a high DC input the size of this link capacitor can be decreased and for small size film or ceramic type capacitors can be used which are not affected by temperature variations. By inserting a transformer in between the input and output provides a physical separation between the input and the output, however, the addition of transformer makes the circuit significantly bulky. Presence of a transformer compromises with the overall efficiency of the circuit due to its losses. High gains have been achieved using coupled inductors or tapped inductors or switched inductor concepts which is always appreciated. However high gains do mean higher voltages and higher currents which ask for devices with high ratings, the result being expensive components and a costly final product. ZSI and qZSI concepts also give high gains however improper selection of inductors and capacitors or switching frequency can result in an unstable circuit and controlling the circuit can be a major challenge. Table 13 summarizes the advantages and disadvantages of the various techniques used in the topologies mentioned in Section 4.

In the fifth segment the most common MPPT algorithms namely HC, P&O and IC were discussed.

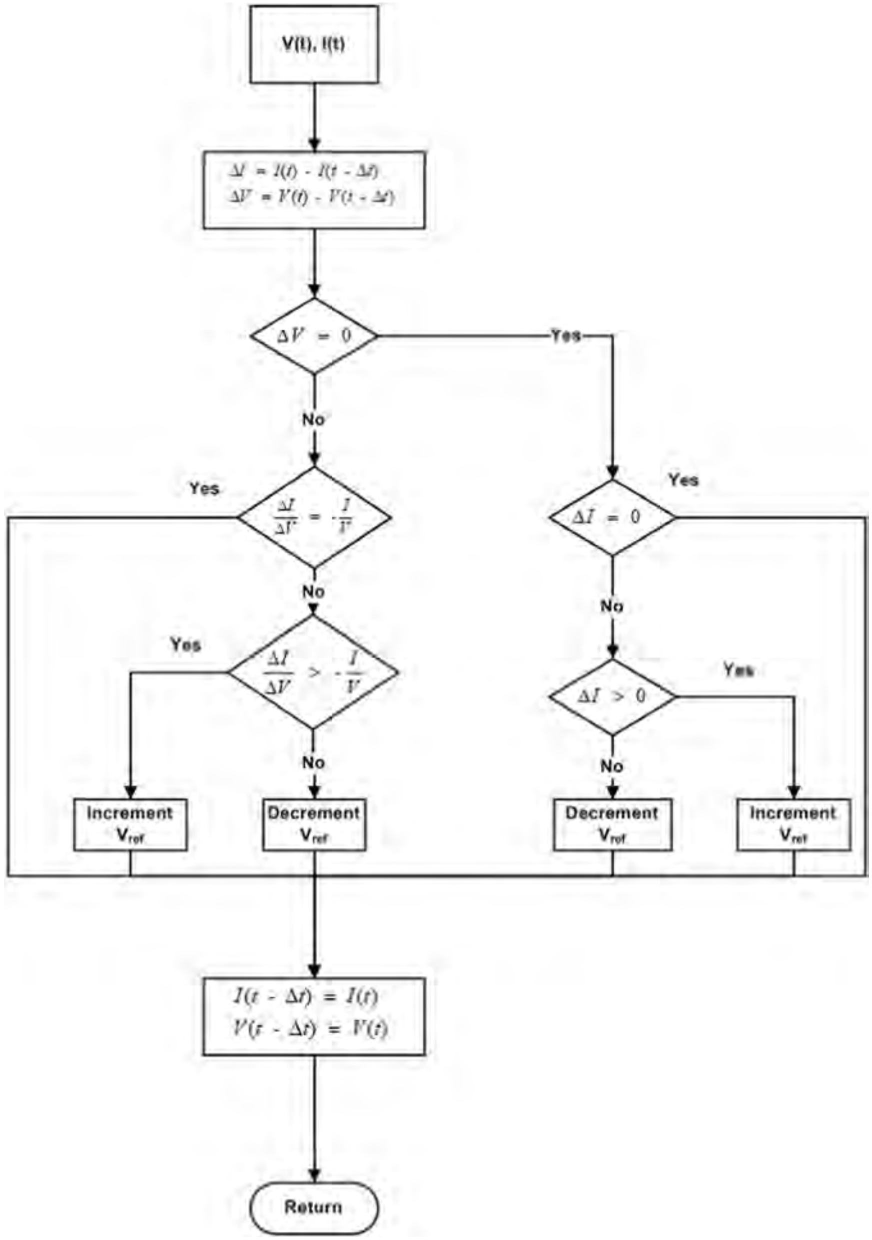

Fig. 44. Flow chart of IC method [97].

Table 13
Advantages and disadvantages of the various techniques mentioned in Section 4.

Technique	Advantage(s)	Disadvantage(s)
High switching frequency	Reduction in the size of passive components such as inductors or capacitors	EMI concerns
DCM operation	DCM operation leads to a high power factor operation	High current stresses on the inductor which asks for higher rating components, low efficiency
CCM operation	Higher efficiency as compared to DCM mode	Can result in core saturation of magnetic components
DC link capacitor	Filters out power pulsation	Lifetime of electrolytic during high-temperature operations
Transformer	Provides a physical separation between input and output	Circuit weight increases, efficiency reduces due to core losses
Coupled inductors or tapped inductors or switched inductor	High gain	Component rating increases, cost increases
ZSI and qZSI	High gain	Improper selection of inductors and capacitors or improper selection of switching frequency leads to an unstable circuit

Acknowledgements

The authors would like to acknowledge the financial support from the Department of Science and Technology (DST), Government of India, Project No. DST/TSG/NTS/2013/59. This work has been carried out in School of Electrical Engineering, VIT University, Vellore, India.

References

[1]. Enerdata_Energy_Statistical_Yearbook_2016.
[2] Kasa N, Iida T, Iwamoto H. Maximum power point tracking with capacitor identifier for photovoltaic power system. IEE Proc Electr Power Appl 2000;147(6):497.
[3] Bose BK, Szezesny PM, Steigerwald RL. Microcontroller control of residential photovoltaic power conditioning system. IEEE Trans Ind Appl 1985;21(5):1182–91.
[4] Kim J-S, Kwon J-M, Kwon B-H. High-efficiency two-stage three-level grid-connected photovoltaic inverter. IEEE Trans Ind Electron 2017;46(c):1.
[5] Barbosa PG, Braga HAC, Barbosa Rodrigues M do Carmo, Teixeira EC. Boost current multilevel inverter and its application on single-phase grid-connected photovoltaic systems. IEEE Trans Power Electron 2006;21(4):1116–24.
[6] Saha S, Sundarsingh VP. Novel grid-connected photovoltaic inverter. Proc Inst Electr Eng 1996;143(2):143–56.
[7] Tian F, Al-Atrash H, Kersten R, Scholl C, Siri K, Batarseh I. A single-staged PV array-based high-frequency link inverter design with grid connection. In: Proceedings of the twenty-first annu. IEEE appl. power electron. conf. expo. 2006. APEC'06; 2006. p. 1451–4.
[8] Mahela OP, Shaik AG. Comprehensive overview of grid interfaced solar photovoltaic systems. Renew Sustain Energy Rev 2017;68(July):316–32.
[9] Jana J, Saha H, Bhattacharya K Das. A review of inverter topologies for single-phase grid-connected photovoltaic systems. Renew Sustain Energy Rev 2016(April):0–1.
[10] Barghi Latran M, Teke A. Investigation of multilevel multifunctional grid connected inverter topologies and control strategies used in photovoltaic systems. Renew Sustain Energy Rev 2015;42:361–76.
[11] Chakraborty S, Hasan MM, Razzak M Abdur. Transformer-less single-phase grid-tie photovoltaic inverter topologies for residential application with various filter circuits. Renew Sustain Energy Rev 2016(January):0–1.
[12] Hasan R, Mekhilef S, Seyedmahmoudian M, Horan B. Grid-connected isolated PV microinverters: a review. Renew Sustain Energy Rev 2017;67:1065–80.
[13] Athari H, Niroomand M, Ataei M. Review and classification of control systems in grid-tied inverters. Renew Sustain Energy Rev 2017;72:1167–76.
[14] Faraji F, Mousavi G SM, Hajirayat A, Birjandi AAM, Al-Haddad K. Single-stage single-phase three-level neutral-point-clamped transformerless grid-connected photovoltaic inverters: topology review. Renew Sustain Energy Rev 2017;80(May):197–214.
[15] Tiwari R, Babu NR. Recent developments of control strategies for wind energy conversion system. Renew Sustain Energy Rev 2016;66:268–85.
[16] Saravanan S, Babu N Ramesh. Maximum power point tracking algorithms for photovoltaic system – a review. Renew Sustain Energy Rev 2016;57:192–204.
[17] Ram JP, Babu TS, Rajasekar N. A comprehensive review on solar PV maximum power point tracking techniques. Renew Sustain Energy Rev 2017;67:826–47.
[18] Calais M, Myrzik J, Spooner T, Agelidis VG. Inverters for single-phase grid connected photovoltaic systems – an overview. In: Proceedings of the 33rd annu. IEEE power electron. spec. conf. 2002. pesc 02. vol. 4; 2002. p. 1995–2000.
[19] Myrzik JMA, Calais M. String and module integrated inverters for single-phase grid connected photovoltaic systems – a review. In: Proceedings of the 2003 IEEE bol. powertech – conf., vol. 2, 2003, p. 430–7.
[20] Kjaer S, Pedersen J, Blaabjerg F. A review of single-phase grid-connected inverters for photovoltaic modules. IEEE Trans Ind Appl 2005;41(5):1292–306. http://dx.doi.org/10.1109/TIA.2005.853371.
[21] Chowdhury A, Razzak M. Single phase grid-connected photovoltaic inverter for residential application with maximum power point tracking. In: Proceedings of the 2013 international conference on informatics, electronics vision (ICIEV); 2013, p. 1–6. 〈http://dx.doi.org/10.1109/ICIEV.2013.6572648〉.
[22] Fraunhofer Gesellschaft Institut fiir Solare Energiesysteme, Course book for the seminar photovoltaic systems, prepared as part of the EU comen project "Sunrise"; 1995.
[23] Meinhardt M, Cramer G. Cost reduction through new PV system technology (Kostenreduktion durch neue PV-Systemtechnik, in German). Kassel, Germany: Kasseler Symposium Energie Systemtechnik, ISET; 2000. p. 152–68.
[24] Meinhardt M, Cramer G. Multi-string-converter – the next step in evolution of the string evolution technology. In: Proceedings of the EPE conference in Graz, Austria; 2001.
[25] Cramer G, Toenges K-H. Modular system technology (string inverters) for grid connected PV sytems in the 100 kW–1 MW power range (Einsatz der modularen Systemtechnik (String-WR) zur Netzkopplung von PV-Anlagen im Leistungsbereich von 100 kW–l MW. in German). In: Proceedings of the 12 symposium photovoltaische Sonnenenergie, Staffelstein, Germany; 1997.
[26] Meinhardt M, Cramer G, Burger B, Zacharias P. Multi-string-converter with reduced specific cost and enhanced functionality. In: Proceedings of the Euro- 2000 conference, Kopenhogen, Denmark; June 2000.
[27] Latran MB, Teke A. Investigation of multilevel multifunctional grid connected inverter topologies and control strategies used in photovoltaic systems. Renew Sustain Energy Rev 2015;42(0):361–76. http://dx.doi.org/10.1016/j.rser.2014.10.030http://www.sciencedirect.com/science/article/pii/S1364032114008478.
[28] Carrasco JM, et al. Power-electronic systems for the grid integration of renewable energy sources: a survey. IEEE Trans Ind Electron 2006;53(4):1002–16.
[29] Xiao B, Hang L, Mei J, Riley C, Tolbert L, Ozpineci B. Modular cascaded h-bridge multilevel pv inverter with distributed mppt for grid-connected applications. IEEE Trans Ind Appl 2015;51(2):1722–31. http://dx.doi.org/10.1109/ TIA.2014.2354396.
[30] Characteristics of the utility interface for photovoltaic (PV) systems. IEC 61727 CDV (Committee Draft for Vote); 2002.
[31] IEEE standard for interconnecting distributed resources with electric power systems, IEEE Std. 1547; 2003.
[32] Limits for harmonic current emission (Equipment input current < 16 A per phase), EN 61000-3-2; 1995.
[33] IEEE Standard 929-2000 (Revision of IEEE Std. 929-1988), IEEE recommended practice for utility interface of photovoltaic (PV) systems, IEEE standards coordinating committee 21, Photovoltaics; 2000.
[34] 〈http://mnre.gov.in/file-manager/UserFiles/Rooftop-Solar-PV-Quality-Standards_Revised.pdf〉. [accessed 31 January 2017].
[35] Chub A, Vinnikov D, Blaabjerg F, Peng FZ. A review of galvanically isolated impedance-source DC-DC converters. IEEE Trans Power Electron 2016;31(4):2808–28.
[36] Sri Revathi B, Prabhakar M. Non isolated high gain DC-DC converter topologies for PV applications – a comprehensive review. Renew Sustain Energy Rev 2016;66:920–33.
[37] Hwu KI, Yau YT. KY converter and its derivatives. IEEE Trans Power Electron 2009;24(1):128–37.
[38] Das M, Agarwal V. Novel high-performance stand-alone solar PV system with high-gain high-efficiency DC–DC converter power stages. In: Proceedings of the IEEE transactions on industry applications, vol. 51, no. 6; Nov.–Dec. 2015. p. 4718–28.
[39] Siwakoti Y, Blaabjerg F. A single switch non-isolated ultra-step-Up DC-DC converter with integrated coupled inductor for high boost applications. IEEE Trans. Power Electron 2017;32(11):8544–58.
[40] Banaei MR, Bonab HAF. A novel structure for single-switch nonisolated transformerless buck–boost DC–DC converter. IEEE Trans Ind Electron 2017;64(1):198–205.
[41] Maheri HM, Babaei E, Sabahi M, Hosseini SH. High step-up DC-DC converter with minimum output voltage ripple. IEEE Trans. Ind. Electron 2017;46(5):3568–75.
[42] Revathi BS, Prabhakar M. Transformerless high-gain DC–DC converter for microgrids. IET Power Electron 2016;9(6):1170–9.
[43] Amirbande M, Yari K, Forouzesh M, Baghramian A. A novel single switch high gain DC-DC converter employing coupled inductor and diode capacitor. In: Proceedings of the 7th power electron. drive syst. technol. conf. (PEDSTC 2016), no. Pedstc; 2016. p. 159–64.
[44] Nag SS, Mishra S. Coupled inductor based high gain current-fed DC-DC bridge converters. In: Proceedings of the 51st annu. meet. IEEE ind. appl. soc. conf. rec. (IAS 2015); 2015. p. 1–6.
[45] Nouri T, Vosoughi N, Hosseini SH, Sabahi M. A novel interleaved non-isolated ultra high step-up DC-DC converter with ZVS performance. IEEE Trans. Ind. Electron 2017;64(5):3650–61.
[46] Ma H, Zhang B, Qiu D, Han J. A novel high gain DC-DC converter with coupled inductor voltage multiplier. In: Proceedings of the 2014 IEEE int. power electron. appl. conf. expo. (PEAC 2014); 2014. p. 16–20.
[47] Feng M, Qu K, Zhao J, Sun M. Non-isolated DC-DC converter with high voltage gain; 2016. p. 2–6.
[48] Cao Y, Samavatian V, Kaskani K, Eshraghi H. A novel non-isolated ultra-high voltage gain DC-DC converter with low voltage stress. IEEE Trans. Ind. Electron 2017;64(4):2809–19.
[49] Sathyan S, Suryawanshi HM, Singh B, Chakraborty C, Verma V, Ballal MS. ZVS-ZCS high voltage gain integrated boost converter for DC microgrid. IEEE Trans Ind Electron 2016;63(11):6898–908.
[50] Baddipadiga B, Ferdowsi M. A high-voltage-gain DC-DC converter based on modified Dickson charge pump voltage multiplier. IEEE Trans. Power Electron 2017;32(10):7707–15.
[51] Ardi H, Ajami A, Kardan F, Nikpour S. Analysis and implementation of a non-isolated bidirectional DC-DC converter with high voltage gain. IEEE Trans. Ind. Electron 2016;63(8):4878–88.
[52] Cáceres RO, Barbi I. A boost DC-AC converter: analysis, design, and experimentation. IEEE Trans Power Electron 1999;14(1):134–41.
[53] Zhou Y, Huang W, Zhao P, Zhao J. Coupled-inductor single-stage boost inverter for grid-connected photovoltaic system. IET Power Electron 2014;7(2):259–70.
[54] Zhao J, Zhao P, Huang W, Zhou Y. Impedance network design and its critical value prediction of tapped-inductor single-stage boost inverter. IET Power Electron 2014;7(6):1618–29.
[55] Kan J, Xie S, Wu Y. Single-stage and boost-voltage grid-connected inverter for fuel-cell generation system. vol. 62, no. 9; 2015. p. 5480–90.
[56] Abramovitz A, Zhao B, Smedley KM. High-gain single-stage boosting inverter for photovoltaic applications. IEEE Trans Power Electron 2016;31(5):3550–8.
[57] Ozcelep Y, Kuntman A, Kuntman H, Yarman S. High voltage stress effects on power MOSFETs in switching DC-DC converters. In: Proceedings of the 2011 int. conf. adv. power syst. autom. prot.; 2011. p. 1278–82.
[58] Peter PK, Agarwal V. Photovoltaic module integrated standalone single stage switched capacitor inverter with maximum power point tracking. IEEE Trans. Power Electron 2017;32(5):3571–84.
[59] Jain S, Agarwal V. A single-stage grid connected inverter topology for solar PV systems with maximum power point tracking. IEEE Trans Power Electron 2007;22(5):1928–40.
[60] Patel H, Agarwal V. A single-stage single-phase transformer-less doubly grounded grid-connected PV interface. IEEE Trans Energy Convers 2009;24(1):93–101.

[61] Abdel-Rahim O, Orabi M, Ahmed ME. Buck-boost interleaved inverter for grid connected photovoltaic system. In: Proceedings of the 2010 IEEE int. conf. power energy PECon2010; 2010. p. 63–8.
[62] Petreus D, Daraban S, Ciocan I, Patarau T, Morel C. Single-stage low cost grid connected inverter in photovoltaic energy applications. In: Proceedings of the 15th international power electron. motion control conf.conf. expo. EPE-PEMC 2012 ECCE Eur.; 2012. p. 1–6.
[63] Lo K-Y, Chen Y-M, Chang Y-R. Bi-directional single-stage grid-connected inverter for battery energy storage system. IEEE Trans. Ind. Electron 2017;64(6):4581–90.
[64] Koushki B, Safaee A, Jain P, Bakhshai A. A step-up/down single-stage ZVS inverter; 2015. p. 2201–6.
[65] Sreekanth T, Mishra MK, Lakshminarasamma N. Coupled inductor-based single-stage high gain DC–AC buck–boost inverter. IET Power Electron 2016;9(8):1590–9.
[66] Inverter SB, Khan AA, Member S, Cha H, Ahmed HF. A highly reliable and high efficiency quasi. vol. 8993, no. c; 2016.
[67] Kumar A, Sensarma P. A 4-switch single-stage single-phase buck-boost inverter. IEEE Trans. Power Electron 2017;32(7):5282–92.
[68] Kasa N, Iida T, Chen L. Flyback inverter controlled by sensorless current MPPT for photovoltaic power system. IEEE Trans Ind Electron 2005;52(4):1145–52.
[69] Shimizu T, Wada K, Nakamura N. A flyback-type single phase utility interactive inverter with low-frequency ripple current reduction on the DC input for an AC photovoltaic module system. In: Proceedings of the 2002 IEEE 33rd annu. ieee power electron. spec. conf. (Cat. No.02CH37289), vol. 3, no. 5; 2002. p. 1483–88.
[70] Hu H, Harb S, Kutkut NH, Shen ZJ, Batarseh I. A single-stage microinverter without using eletrolytic capacitors. IEEE Trans Power Electron 2013;28(6):2677–87.
[71] Chen Z, Li M, Wu Q, Xu Y. A single-stage grid-connected flyback inverter with power decoupling function. In: Proceedings of the 2015 IEEE appl. power electron. conf. expo. (APEC); 2015. p. 2946–52.
[72] Zeng J, Qiao W, Wei C, Qu L. A soft-switched three-port single-stage inverter for photovoltaic-battery systems; 2015. p. 4568–73.
[73] Abdel-rahim O, Funato H, Haruna J. Pseudo single stage flyback current source inverter for grid connected PV applications. In: Proceedings of the 41st annu. conf. ieee ind. electron. soc. (IECON 2015); 2015. p. 1–6.
[74] Prasad BS, Jain S, Agarwal V. Universal single-stage grid-connected inverter. IEEE Trans Energy Convers 2008;23(1):128–37.
[75] De Lima RR et al. Design and modeling of a transformerless hybrid inverter system using a fuel cell as energy storage element for microgrids with sensitive loads. In: Proceedings of the 2015 IEEE 6th int. symp. power electron. distrib. gener. syst. (PEDG 2015), no. 1; 2015.
[76] Pan C-T, Cheng M-C, Lai C-M. A novel integrated DC/AC converter with high voltage gain capability for distributed energy resource systems. IEEE Trans Power Electron 2012;27(5):2385–95.
[77] Darwish A, Holliday D, Ahmed S, Massoud AM, Williams BW. A single-stage three-phase inverter based on Cuk converters for PV applications. IEEE J Emerg Sel Top Power Electron 2014;2(4):797–807.
[78] Mehrnami S, Mazumder SK. Discontinuous modulation scheme for a differential-mode Cuk inverter. IEEE Trans Power Electron 2014;30(3):1–13.
[79] Gautam V, Kumar A, Sensarma P. A novel single stage, transformerless PV inverter; 2014. p. 907–12.
[80] Chamarthi P, Rajeev M, Agarwal V. A novel single stage zero leakage current transformer-less inverter for grid connected PV systems. In: Proceedings of the 2015 IEEE 42nd photovoltaic specialist conference (PVSC), New Orleans, LA; 2015. p. 1–5.
[81] Peng Fang Zheng. Z-source inverter. IEEE Trans Ind Appl 2003;39(2):504–10.
[82] Nguyen MK, Lim YC, Kim YG. TZ-source inverters. IEEE Trans Ind Electron 2013;60(12):5686–95.
[83] Ge B, et al. An energy-stored quasi-Z-source inverter for application to photovoltaic power system. IEEE Trans Ind Electron 2013;60(10):4468–81.
[84] Nguyen M-K, Lim Y-C, Choi J-H. Two switched-inductor quasi-Z-source inverters. IET Power Electron 2012(7):1017–25.
[85] Ho AV, Chun TW, Lee HH, Kim HG. Active switched quasi-Z-source inverter with high-boost ability for low-voltage renewable energy sources. In: Proceedings of the 5th int. conf. clean electr. power renew. energy resour. impact (ICCEP 2015). no. 2; 2015. p. 627–32.
[86] Erickson RW, Maksimovic D. Soft switching. Fundamentals of power electronics. India: Springer; 2010. p. 761–85.
[87] Cossutta P, Aguirre MP, Cao A, Raffo S, Valla MI. Single-stage fuel cell to grid interface with multilevel current-source inverters. IEEE Trans Ind Electron 2015;62(8):5256–64.
[88] Surapaneni RK. A single-stage CCM Zeta micro sol photovolt AC (PVAC) modul. vol. 3, no 4; 2015. p. 3271–7.
[89] Kumar A, Gautam V, Sensarma P. A SEPIC derived single stage buck-boost inverter for photovoltaic applications. Proc IEEE Int Conf Ind Technol 2014:403–8.
[90] Casadei D, Grandi G, Rossi C. Single-phase single-stage photovoltaic generation system based on a ripple correlation control maximum power point tracking. IEEE Trans Energy Convers 2006;21(2):562–8. http://dx.doi.org/10.1109/TEC.2005.853784.
[91] Kuo C-L, Lin C-H, Yau H-T, Chen J-L. Using self-synchronization error dynamics formulation based controller for maximum photovoltaic power tracking in micro-grid systems. IEEE J Emerg Sel Top Circuits Syst 2013;3(3):459–67. http://dx.doi.org/10.1109/JETCAS.2013.2272839.
[92] Veerachary M, Senjyu T, Uezato K. Maximum power point tracking control of IDB converter supplied PV system. IEEE Proc Electron Power Appl 2001:494–502.
[93] Weidong X, Dunford WG. A modified adaptive hill climbing MPPT method for photovoltaic power systems. IEEE Power Electron Spec Conf 2004;35:1957–63.
[94] Liu Fangrui, Kang Yong, Zhang Yu and Duan Shanxu. Comparison of P&O and hill climbing MPPT methods for grid-connected pv converter. In: Proceedings of the 3rd IEEE conference on industrial electronics and applications (ICIEA); 2008.
[95] Nicola Femia, Giovanni Petrone, Giovanni Spagnuolo. Optimization of perturb and observe maximum power point tracking method. IEEE Trans Power Electron 2005;20(4):963–73.
[96] Mellit A, Rezzouk H, Messai A, Medjahed B. FPGA-based real time implementation of MPPT-controller for photovoltaic systems. Renew Energy 2011;36(5):1652–61.
[97] Trishan Esram, Chapman Patrick L. Comparison of photo voltaic array maximum power point tracking techniques. IEEE Trans Energy Convers 2007;22(2):439–49.